METHODS

Cells, virus and other reagents. Monkey Vero cells were cultured in αMEM containing 15% FBS. MEFs and human 293T cells were cultured in DMEM containing 10% FBS. Human Namalwa cells were maintained in RPMI1640 containing 10% FBS. *DNase II*$^{-/-}$ MEFs expressing $\alpha_v\beta_3$-integrin (*DNase II*$^{-/-}$ MEFs/integrin) were described previously[4]. *DNase II*$^{-/-}$ *Irf3*$^{-/-}$ *Irf7*$^{-/-}$ MEFs were established from embryonic day (E)13.5 *DNase II*$^{-/-}$ *Irf3*$^{-/-}$ *Irf7*$^{-/-}$ mouse embryos as described[4]. To prepare the fetal liver macrophages, the liver from E14.5 mouse embryo was dissected and passed through a 22-gauge needle five times. After washing with PBS, the cells were cultured in αMEM containing 10% FBS supplemented with 10% (v/v) supernatant of CMG14-12 cells producing mouse macrophage colony-stimulating factor[30]. After 48 h, the cells were washed, and adherent cells were used as fetal liver macrophages. NDV was provided by T. Fujita (Kyoto University) and propagated in fertilized chicken eggs as described[31]. VSV (Indiana strain) was propagated in mouse L929 cells.

Antibodies used were mouse monoclonal antibodies against Flag (M2 antibody, Sigma), HA (clone 12C5, Boehringer Mannheim; clone 16B12, Babco), PARP (BD), and anti-tubulin (EMD Chemicals), rabbit polyclonal antibodies against IRF3 (Zymed Laboratories) and IPS-1 (Cell Signaling), and rabbit monoclonal antibody against phosphorylated-IRF3 (Ser 396; Cell Signaling).

Leucine zipper-tagged human Fas ligand[32] and mouse MFG-E8 (ref. 33) were produced in monkey COS7 and human 293T cells, respectively. Poly(I:C) was purchased from GE Healthcare. Calf thymus DNA, *E. coli* DNA and LPS were from Sigma. A phosphorothioate-stabilized CpG oligonucleotide[34] of 5′-TCCATGACGTTCCTGATGCT-3′ was purchased from Hokkaido System Science.

Production of monoclonal antibody against mouse EYA4. To produce monoclonal antibody against mouse EYA4, the N-terminal domain of EYA4 (amino acids 2–346) was joined to maltose-binding protein (MBP) using pMAL-p2X vector (New England BioLab), or to glutathione-*S*-transferase (GST) using pGEX-5X-1 vector (GE Healthcare). MBP–EYA4 and GST–EYA4 were produced in *E. coli* BL21(DE3) pLysS strain, and purified using Amylose-resin (New England BioLab) and glutathione-sepharose (GE Healthcare), respectively. Armenian hamsters were immunized by subcutaneously injecting four times with 50 μg of MBP–EYA4 in a 2-week interval. For the first injection, MBP–EYA4 was mixed with complete Freund's adjuvant (DIFCO), while it was mixed with incomplete Freund's adjuvant for the second to fourth injections. A final injection with 50 μg MBP-EYA4 was given into the foot pads. Two days later, popliteal and inguinal lymph nodes were collected, and the lymphocytes were fused with mouse myeloma NSO cell line[35]. Hybridomas were selected in HAT medium (Boehringer Ingelheim), and the supernatants were tested by ELISA for their ability to recognize GST–EYA4. Positive clones were examined for their suitability in western blotting, and one hybridoma (clone 5-7C 48) was subjected to limiting dilution. The hybridoma was grown in GIT medium (Nihon Pharmaceutical), and the antibodies were purified by protein A-sepharose.

Expression cloning. Poly(A) RNA was prepared from MEFs using an mRNA purification kit (GE Healthcare). Double-stranded cDNA was generated with the SuperScript Choice System (Invitrogen). cDNAs longer than 0.5 kb were ligated into a BstXI-digested pMXs vector[36] using the BstXI adaptor, and introduced into *E. coli* DH10B by electroporation, to generate a cDNA library of about 20,000 clones. The library was divided into 400 pools of 50 clones, and plasmid DNA was prepared from each pool using NucleoSpin Multi-96 Plus Plasmid (Macherey-Nagel). The DNA was introduced into Plat-E packaging cells[37], and the culture supernatant was used to infect *DNase II*$^{-/-}$ MEFs/integrin. At 48 h after the infection, the MEFs were allowed to engulf apoptotic *Cad*$^{-/-}$ thymocytes, and the concentration of CXCL10 in the culture supernatant was determined by ELISA. The pools that gave a positive result were subjected to sib-selection.

Engulfment of apoptotic cells and transfection of DNA. The MFG-E8-dependent engulfment of apoptotic cells was performed as described[33]. In brief, thymocytes from *Cad*$^{-/-}$ mice were treated for 2 h with Fas ligand to induce apoptosis in about 50% of the cell population. The apoptotic cells were added to MEFs at a ratio of 50:1, and incubated for 20 h in the presence of 0.1 μg ml^{-1} MFG-E8.

To introduce nucleic acids into cells, the nucleic acids were preincubated at room temperature for 15 min with FuGENE6 transfection reagent (Roche Diagnostics) at a ratio of 1:1.5 (w/v) in DMEM, added to the cells, and incubated at 37 °C for 6 (for macrophages) or 12 (for MEF and 293T) h.

Enzyme-linked immunosorbent assay. The concentrations of IFN-β and CXCL10 were determined by ELISAs using the mouse Interferon Beta ELISA Kit (PBL) and mouse CXCL10 DuoSet ELISA Development system (R&D), respectively. Streptavidin-conjugated horseradish peroxidase (HRP) or alkaline phosphatase was used as the substrate. In some cases, signals were amplified with the AmpliQ (Dako) detection system.

Real-time PCR. Total RNA was prepared from cells using the RNeasy kit with the RNase-Free DNase set (Qiagen). After reverse-transcription with oligo(dT) primer using a Transcriptor First Strand cDNA Synthesis Kit (Roche Diagnostics), aliquots of the products were amplified using the LightCycler 480 system (Roche Diagnostics) according to the instructions provided by the manufacturer. The primers used for the mouse genes were as follows: *Ifnb*, 5′-CCACCACAGCCCTCTCCATCAACTAT-3′ and 5′-CAAGTGGAGAGCAG TTGAGGACATC-3′; *Cxcl10*, 5′-CCATCAGCACCATGAACCCAAGT-3′ and 5′-CACTCCAGTTAAGGAGCCCTTTTAGACC-3′; β-actin, 5′-TGTGATGGT GGGAATGGGTCAG-3′, and 5′-TTTGATGTCACGCACGATTTCC-3′. The primers for the human genes were as follows: *IFNB*, 5′-CCAACAA GTGTCTCCTCCAAA-3′ and 5′-CCTCAGGGATGTCAAAGTTCA-3′; *EYA1*, 5′-AGGCACCATACAGCTACCAGAT-3′ and 5′-GCTGGTCATATAATGTGC TGGA-3′; *EYA2*, 5′-GGCACTAAACCTCATCAACTCC-3′ and 5′-CACCACG TAGACAGCTTTTCTG-3′; *EYA3*, 5′-CCAGATGTCAGTGATCAGAAGC-3′ and 5′-GGGTAGACAGCATAGGGTTGAG-3′; *EYA4*, 5′- CGCTTGTGTACGC TATTTGTTGT-3′ and 5′-TTTTCTCACTTCTCCTGCCACTC-3′; β-actin, 5′-GCATCCTCACCCTGAAGTAC-3′ and 5′-CTTAATGTCACGCACGATT TC-3′.

Expression plasmid. The cDNAs of mouse EYA1 (GenBank accession NP_034294), EYA2 (GenBank accession NP_034295), EYA3 (GenBank accession NP_034296), and EYA4 (GenBank accession NP_034297) were isolated by RT–PCR from the RNA of MEFs, and their authenticity was confirmed by DNA sequencing. As the N- and C-terminal regions of EYA3, amino acids 2–255 (encoded by exons 2–10), and amino acids 256–526 (encoded by exons 11–18), were used, respectively. Whereas amino acids 2–345 (encoded by exons 2–11), and amino acids 346–616 (encoded by exons 12–19), were used as the N- and C-terminal regions of EYA4, respectively. In the EYA4-Y4 mutant, tyrosine was replaced by alanine at four positions (amino acids 258, 261, 262 and 267). The EYA4-DYY mutant was produced by replacing Asn at position 246 and two Tyr residues at positions 247 and 250 with Ala. In the Asp352Asn mutant, the Asp at position 352 was replaced with Asn. The expression plasmid for these mutants were constructed by recombinant PCR[38]. All EYA proteins and their derivatives were Flag-tagged at the N terminus.

Mouse cDNAs for *Ips-1* (GenBank accession NP_659137), *Trif* (GenBank accession NP_778154), *Sting* (GenBank accession XP_905219), *Nlrx1* (GenBank accession NP_848507), *Irf3* (GenBank accession NP_058545), *Six4* (GenBank: NP_035512) and *MyD88* (GenBank: NP_034981) were isolated by RT–PCR from the RNA of MEF or fetal liver macrophages. Each cDNA was tagged with three tandem haemagglutinins (a peptide of influenza haemagglutinin, YPYDVPDYA) at the N terminus (IPS-1, TRIF, SIX4, NLRX1 and MyD88) or the C terminus (STING), or with Flag at the N terminus (IRF3).

Production of recombinant EYA proteins. The mouse EYA proteins were produced by transfecting human 293T cells with the respective expression plasmids, and the accumulated protein was purified using anti-Flag M2 affinity gel (Sigma). In brief, the expression vectors for Flag-tagged EYA and its derivatives were generated in pEF-BOS vector[39] and introduced into human 293T cells using the calcium-phosphate co-precipitation method. Sixty to seventy-two hours later, the cells were lysed by incubating them for 30 min at 4 °C in 50 mM Tris-HCl (pH 7.4) containing 1.0% (v/v) NP40, 150 mM NaCl, 2 mM EDTA, 2 mM EGTA, 2.0 μg ml^{-1} pepstatin, 2.0 μg ml^{-1} leupeptin, 2 μg ml^{-1} aprotinin, and 2 μM *p*ABSF (4-(2-aminoethyl)-benzenesulfonyl fluoride hydrochloride). After removing the cell debris by centrifugation at 39,800*g* for 40 min, the cell extracts were affinity-purified with anti-Flag-Sepharose (M2, Sigma), and the protein was eluted with 50 mM Tris-HCl buffer (pH 7.4) containing 100 μg ml^{-1} of Flag peptide (Sigma), 150 mM NaCl, and 0.1% NP40.

Recombinant EYA3 and EYA4 were also produced *in vitro* using the wheat-germ cell-free system[40]. In brief, the DNA fragment for the Flag-tagged EYA3 or EYA4 was inserted into pEU E01 vector (Cell Free Science). With the resultant plasmid as a template, *Eya3* or *Eya4* mRNA was synthesized with SP6 RNA polymerase using a kit from Cell Free Sciences according to the instructions provided by the manufacture. EYA protein was then synthesized with the mRNA by incubation at 15 °C for 20 h with 250 μl of wheat-germ extracts and 5.5 ml of SUM-AMIX (Cell Free Sciences). After incubation, the reaction mixture was diluted eightfold with 50 mM Tris-HCl (pH 7.4) containing 1.0% NP40, 150 mM NaCl, 2 mM EDTA, 2 mM EGTA, 2.0 μg ml^{-1} pepstatin, 2.0 μg ml^{-1} leupeptin, 2 μg ml^{-1} aprotinin and 2 μM *p*ABSF, and the Flag-tagged EYA protein was purified using anti-Flag-Sepharose as described earlier.

Assay for phosphatase activity. The phosphorylated synthetic peptides KR(pS)IRR, KR(pT)IRR, RRA(pT)VA and END(pY)INASL were custom-synthesized by the Toray Research Center, and KR(pT)IRR, DLDVPIPGRF DRRV(pT)VAAE, SDQEKRKQI(pT)VRGL, LDPRQVEMIRRRRP(pT)PAML, (pT)EEEEE, (pS)EEEEE, DADE(pY)LIPQQG, END(pY)INASL, RRLIEDAE (pY)AARG, TRDI(pY)ETDYYRK and DRV(pY)IHPF were custom-synthesized

by MBL. YSPTSPS(pY)SPTSPS, YSPTSPSY(pS)PT(pS)PS and YSPTSPSY SP(pT)SPS were custom-synthesized by Invitrogen. Sodium orthovanadate, okadaic acid and calyculin A were purchased from EMD Chemicals. Recombinant human protein phosphatase 2A, 2B and 2C were purchased from Wako, Promega and EMD Chemicals, respectively.

To assay the phosphatase activity, the recombinant EYA was incubated in a final volume of 50 µl with 400 µM phosphorylated peptide at 37 °C for 60 min in 50 mM MES-KOH buffer (pH 6.0) containing 2 mM $MgCl_2$ and 50 µM dithiothreitol (DTT) for the tyrosine phosphatase or in 50 mM Tricine-KOH buffer (pH 8.0) containing 5 mM EDTA and 50 µM DTT for the serine/threonine-phosphatase. The phosphatase activity of human protein phosphatase 2A, 2B and 2C was assayed similarly by incubating at 37 °C for 60 min. The buffer was essentially as previously reported[41,42]. That is, 50 mM Tris-HCl buffer (pH 7.0) containing 0.1 mM EGTA and 14.2 mM 2-mercaptoethanol for protein phosphatase 2A, 50 mM HEPES-KOH buffer (pH 7.5) containing 2 mM $NiCl_2$ for protein phosphatase 2B, and 50 mM Tris-HCl buffer (pH 7.5) containing 0.1 mM EDTA, 30 mM $MgCl_2$ and 1 mM DTT for protein phosphatase 2C. The released phosphate was quantified by a colourimetric method using the malachite green-molybdate as described[43]. In brief, the reaction was terminated by the addition of 50 µl of H_2O and 20 µl of 1.75% (w/v) ammonium molybdate·$4H_2O$ in 6.0 N H_2SO_4, and incubated at room temperature for 20 min. A solution (20 µl) containing 0.35% (w/v) malachite green and 0.35% (w/v) polyvinylalcohol (molecular mass 13,000–23000 Da) was added to the reaction mixture, which was further incubated for 20 min at room temperature. The malachite green-ammonium molybdate phosphate complex was detected at 620 nm using a Micro Plate Reader (BioLumin 960). K_m and K_{cat} values for the phosphatase activities of EYA were determined using Hanes-Woolf Plot.

Stable cell transformants. To express EYA and IRF3 in mouse MEFs and fetal liver macrophages, the corresponding cDNA was introduced into pMXs vector[36]. Retrovirus was prepared by transfecting PlatE packaging cells[37] with the expression vector, and used to infect MEF and macrophages[4]. To establish Namalwa cells that constitutively express mouse EYA4, the Flag-tagged EYA4 cDNA was introduced into pEF-BOS vector[39] to generate pEF-Flag-EYA4. Namalwa cells were co-transfected by electroporation with Aat II-digested pEF-Flag-EYA4 and a plasmid carrying the hygromycin-resistant gene. After being selected with 1.0 mg ml^{-1} hygromycin, the clones expressing EYA4 were identified by western blotting with anti-Flag antibody.

Cytopathic assay for VSV. Samples carrying VSV were seriously diluted, and incubated at 37 °C for 40 h with 1×10^4 Vero cells in 96-well microtitre plate. After incubation, surviving cells were stained with 0.5% crystal violet, and dissolved in methanol. Absorbance at 595 nm was determined using an ELISA reader (Infinite 2000, TECAN).

shRNA. shRNA expression plasmids for human *EYA1*, *EYA2*, *EYA3* and *EYA4* in a pRS shRNA vector carrying a puromycin-resistance gene were purchased from OriGene. The target sequences for the shRNAs were as follows: for human *EYA1*, 5′-ATCTGGCATCACCAGCCAAGCAGTTACAG-3′; for human *EYA2*, 5′-CC GAGTCACTTGCTGGTGAATACAACACA-3′; for human *EYA3*, 5′-AGT AGCCAGCATCTCAAACCAGGATTATC-3′; for human *EYA4*, 5′-CCTG AGGTTTGAATCTGACTTTAGCCTAC-3′; and for the control GFP, 5′-TGAC CACCCTGACCTACGGCGTGCAGTGC-3′. The U6-EYA1 and U6-EYA2 portions were joined into one pRS vector, and the U6-Eya3 and U6-EYA4 potions were joined into another pRS vector. Human 293T cells were transfected using the Fugene transfection reagent with the two shRNA plasmids. Sixty hours later, the cells were transfected with poly(I:C), and the *Ifnb* mRNA was quantified.

Luciferase assay. The promoter activity was determined by luciferase assay using the Dual-Luciferase Reporter Assay System (Promega). In brief, a DNA fragment carrying the mouse *Ifnb* promoter region (−121 to +22: +1, transcription start site)[44] was amplified by PCR from mouse genomic DNA. The mouse myogenin promoter (−182 to +52)[45] was provided by A. Sehara-Fujisawa (Kyoto University). The *Ifnb* and myogenin promoter was inserted upstream of the firefly luciferase gene of pGL3 to generate pGL3-mIFNβ125luc and pGL3MG-185, respectively. The expression vector for EYA4, IPS-1, TRIF, MyD88 or Six4 cDNA in pEF-BOS was introduced into MEF or 293T cells together with pGL3-mIFNβ125luc or pGL3MG-185 reporter plasmid. Twenty-four (for *Ifnb* promoter) or forty-eight (for myogenin promoter) hours later, the luciferase activity was determined as described previously[46]. pEF-Rluc or pSV-Rluc, which carries the *Renilla* luciferase gene downstream of the elongation factor 1 promoter[46] or SV40-early promoter, was used as an internal control for transfection.

Electrophoretic mobility shift assay. For the EMSAs, nuclear extracts were prepared as described[47]. The probe DNA carrying the NF-κB binding site (5′-AGTTGAGGGGACTTTCCCAGG-3′) was labelled with biotin using a biotin 3′ end DNA labelling kit (Pierce). For the binding reaction, nuclear extracts (2 µg protein) were incubated for 30 min at 25 °C with 20 fmol of biotin-labelled probe in 10 µl of a reaction mixture containing 10 mM Tris-HCl (pH 7.5), 50 mM KCl, 1 mM DTT, 5% glycerol, 2% polyvinylalcohol, and 500 ng poly(I:C) in the presence or absence of 4 pmoles of unlabelled probe. The reaction mixture was separated by electrophoresis on a 6% polyacrylamide gel in 50 mM Tris-HCl (pH 8.5) containing 380 mM glycine, and 2 mM EDTA, and the shifted band was detected with the LightShift Chemiluminescent EMSA Kit (Pierce).

Fractionation of the cell extracts. The cell extracts were fractionated into nuclear and cytoplasmic fractions as described previously[47]. In brief, MEFs were incubated at 4 °C for 10 min in hypotonic buffer (10 mM HEPES-KOH buffer (pH 7.9), 0.1 mM EDTA, 0.1 mM EGTA, 1 mM DTT, 10 mM KCl and a cocktail of protease inhibitors and phosphatase inhibitors (Roche Diagnostics) to allow cells to swell. The cells were then lysed by vigorously vortexing in the hypotonic buffer containing 6% sucrose and 0.1% NP-40. The lysates were spun at 14,000*g* for 2 min, and the supernatants were used as the cytoplasmic fraction. The pellets were suspended in 20 mM HEPES-KOH (pH 7.9) containing 0.2 mM EDTA, 2 mM EGTA, 2 mM DTT, 25% glycerol, 420 mM NaCl, and a cocktail of protease inhibitors and phosphatase inhibitors. After incubating at 4 °C for 30 min, the mixture was spun at 87,920*g* for 30 min, and the supernatants were used as nuclear extracts.

Immunoprecipitation and western blotting. Human 293T cells (2×10^6 cells) were transfected by the calcium-phosphate precipitation method with a total of 16 µg of expression plasmids for Flag-tagged or HA-tagged protein. Cells were collected 30 h after the transfection and lysed in lysis buffer containing 50 mM Tris-HCl (pH 8.0), 1% NP-40, 150 mM NaCl, 5 mM EDTA, and a cocktail of protease inhibitors and phosphatase inhibitors (Roche Diagnostics). Cell lysates were precleared by incubating at 4 °C with Sepharose CL-4B (Sigma) for 2 h, and then incubated with anti-Flag M2 affinity gel for 2 h. After washing with the lysis buffer, the proteins bound to the beads were eluted by boiling in SDS sample buffer (62.5 mM Tris-HCl (pH 6.8), 2% SDS, 10% glycerol, 5% 2-mercaptoethanol, and 0.001% bromphenol blue), separated by electrophoresis on a 10% or 10–20% polyacrylamide gel, and transferred onto a PVDF membrane. The membrane was incubated with biotin-conjugated mouse anti-Flag, or mouse anti-HA (clone 12CA5), followed by incubation with HRP-conjugated streptavidin (Roche Diagnostics). The peroxidase activity was detected by Immobilon Western ECL system (Millipore). In some case, cells were lysed with SDS sample buffer, and directly subjected to SDS–PAGE, followed by western blotting.

For analysis by native PAGE[14], cells were suspended in 50 mM Tris-HCl (pH 7.5) containing 150 mM NaCl, 1 mM EDTA, 2% NP-40, cocktails of protease inhibitors and phosphatase inhibitors (Roche Diagnostics). After being briefly vortexed, the mixture was spun for 10 min at 17,600*g*, and the supernatant (3 µg protein) was separated by electrophoresis at 20 mA on a 7.5% polyacrylamide gel (Bio-Rad) in 62.5 mM Tris-HCl buffer (pH 6.8) containing 15% glycerol and 1% deoxycholate, and transferred to a PVDF membrane for western blotting analysis.

30. Takeshita, S., Kaji, K. & Kudo, A. Identification and characterization of the new osteoclast progenitor with macrophage phenotypes being able to differentiate into mature osteoclasts. *J. Bone Miner. Res.* 15, 1477–1488 (2000).
31. Lam, K. M. & Hao, Q. Induction of lymphocyte agglutination and lysis by Newcastle disease virus. *Vet. Microbiol.* 15, 49–56 (1987).
32. Shiraishi, T. *et al.* Increased cytotoxicity of soluble Fas ligand by fusing isoleucine zipper motif. *Biochem. Biophys. Res. Commun.* 322, 197–202 (2004).
33. Hanayama, R. *et al.* Identification of a factor that links apoptotic cells to phagocytes. *Nature* 417, 182–187 (2002).
34. Hemmi, H. *et al.* A Toll-like receptor recognizes bacterial DNA. *Nature* 408, 740–745 (2000).
35. Ray, S. & Diamond, B. Generation of a fusion partner to sample the repertoire of splenic B cells destined for apoptosis. *Proc. Natl Acad. Sci. USA* 91, 5548–5551 (1994).
36. Kitamura, T. *et al.* Retrovirus-mediated gene transfer and expression cloning: powerful tools in functional genomics. *Exp. Hematol.* 31, 1007–1014 (2003).
37. Morita, S., Kojima, T. & Kitamura, T. Plat-E: an efficient and stable system for transient packaging of retroviruses. *Gene Ther.* 7, 1063–1066 (2000).
38. Higuchi, R. in *PCR Protocols: a Guide to Methods and Applications* 177–188 (Academic, 1990).
39. Mizushima, S. & Nagata, S. pEF-BOS, a powerful mammalian expression vector. *Nucleic Acids Res.* 18, 5322 (1990).
40. Sawasaki, T., Ogasawara, T., Morishita, R. & Endo, Y. A cell-free protein synthesis system for high-throughput proteomics. *Proc. Natl Acad. Sci. USA* 99, 14652–14657 (2002).
41. Donella Deana, A. *et al.* An investigation of the substrate specificity of protein phosphatase 2C using synthetic peptide substrates; comparison with protein phosphatase 2A. *Biochim. Biophys. Acta* 1051, 199–202 (1990).
42. Umeda, I. O., Nakata, H. & Nishigori, H. Identification of protein phosphatase 2C and confirmation of other protein phosphatases in the ocular lenses. *Exp. Eye Res.* 79, 385–392 (2004).
43. Van Veldhoven, P. P. & Mannaerts, G. P. Inorganic and organic phosphate measurements in the nanomolar range. *Anal. Biochem.* 161, 45–48 (1987).
44. Yoneyama, M. *et al.* Direct triggering of the type I interferon system by virus infection: activation of a transcription factor complex containing IRF-3 and CBP/p300. *EMBO J.* 17, 1087–1095 (1998).

45. Fujisawa-Sehara, A., Hanaoka, K., Hayasaka, M., Hiromasa-Yagami, T. & Nabeshima, Y. Upstream region of the myogenin gene confers transcriptional activation in muscle cell lineages during mouse embryogenesis. *Biochem. Biophys. Res. Commun.* 191, 351–356 (1993).
46. Kawane, K. *et al.* Structure and promoter analysis of murine CAD and ICAD genes. *Cell Death Differ.* 6, 745–752 (1999).
47. Shapiro, D. J., Sharp, P. A., Wahli, W. W. & Keller, M. J. A high-efficiency HeLa cell nuclear transcription extract. *DNA* 7, 47–55 (1988).

Biochemical and Biophysical Research Communications 378 (2009) 186–191

Contents lists available at ScienceDirect

Biochemical and Biophysical Research Communications

journal homepage: www.elsevier.com/locate/ybbrc

Adenovirus-mediated gene transfer of adiponectin reduces the severity of collagen-induced arthritis in mice

Kosuke Ebina [a,b], Kazuya Oshima [a], Morihiro Matsuda [b,c,d], Atsunori Fukuhara [b], Kazuhisa Maeda [b], Shinji Kihara [b], Jun Hashimoto [a], Takahiro Ochi [e], Nirmal K. Banda [f], Hideki Yoshikawa [a], Iichiro Shimomura [a,*]

[a] Departments of Orthopaedics and Metabolic Medicine, Graduate School of Medicine, Osaka University, 2-2 Yamadaoka, Suita, Osaka 565-0871, Japan
[b] Metabolic Medicine, Graduate School of Medicine, Osaka University, 2-2 Yamadaoka, Suita, Osaka 565-0871, Japan
[c] Division of Analysis for Pathophysiology, Institute of Clinical Research, National Hospital Organization Kure Medical Center, Kure, Hiroshima 737-0023, Japan
[d] Department of Internal Medicine, National Hospital Organization Kure Medical Center, Kure, Hiroshima 737-0023, Japan
[e] Osaka Police Hospital, 10-31 Kitayama-cho, Tennoji-ku, Osaka 543-0035, Japan
[f] Division of Rheumatology B115, University of Colorado at Denver and Health Sciences Center, M-20 3104, 1775 North Ursula St., Aurora, CO 80045, USA

ARTICLE INFO

Article history:
Received 24 October 2008
Available online 21 November 2008

Keywords:
Adiponectin
Collagen-induced arthritis
Complement
Disease severity
Inflammation
Mice
Rheumatoid arthritis

ABSTRACT

Adiponectin (APN) is a hormone released by adipose tissue with anti-inflammatory properties. The purpose of this study was to examine the therapeutic effects of systemic delivery of APN in murine arthritis model. Collagen-induced arthritis (CIA) was induced in male DBA1/J mice, and adenoviral vectors encoding human APN (Ad-APN) or beta-galactosidase (Ad-β-gal) as control were injected either before or during arthritis progression. Systemic APN delivery at both time points significantly decreased clinical disease activity scores of CIA. In addition, APN treatment before arthritis progression significantly decreased histological scores of inflammation and cartilage damage, bone erosion, and mRNA levels of pro-inflammatory cytokines in the joints, without altering serum anti-collagen antibodies levels. Immunohistochemical staining showed significant inhibition of complement C1q and C3 deposition in the joints of Ad-APN infected CIA mice. These results provide novel evidence that systemic APN delivery prevents inflammation and joint destruction in murine arthritis model.

Rheumatoid arthritis (RA) is an autoimmune disease characterized by chronic inflammation of joint synovial tissues, followed by cartilage destruction and bone erosion. Collagen-induced arthritis (CIA) is an established rodent model of autoimmune polyarthritis with many similarities to human RA, and the immunopathological process of CIA has been reported in details [1]. Briefly, injection of chicken type II collagen (CII) in complete Freund's adjuvant (CFA) results in proliferation and differentiation of T-cells into CD4+Th1-cells in the draining lymph nodes. These cells then promote the production of anti-collagen IgG by activated CII-specific B-cells. These antibodies enter the joint and bind to CII, forming an immunocomplex (IC), which activates the complement cascade. Complement enhances the permeability of the vascular endothelium, and facilitates infiltration of monocytes (macrophages) and neutrophils into the joint. In the joint space, macrophages produce tumor necrosis factor (TNF)-α and interleukin (IL)-1. TNF-α enhances vascular permeability and migration of inflammatory cells into the joint space, and IL-1 is the primary trigger of tissue destruction by infiltrating cells and resident synoviocytes.

Adiponectin (APN) is an adipocytokine that shares strong homologies with the complement factor C1q and TNF-α [2]. APN has anti-inflammatory effects, and suppresses TNF-α and IL-6 production by macrophages activated with lipopolysaccharide (LPS) through suppression of nuclear factor-kappa B (NF-κB) signaling [3]. Accumulating evidence suggests a novel link between APN and inflammatory joint diseases. For example, APN concentration in the synovial fluid correlates negatively with synovial fluid leukocyte count in patients with RA, suggesting that APN is an anti-inflammatory molecule in RA [4]. However, APN levels in synovial fluid and serum are elevated in patients with RA compared with healthy controls [4], and APN treatment induces IL-6 production by synovial fibroblasts from RA patients [5], suggesting that APN is a pro-inflammatory molecule in RA. Thus, the effects of APN in RA are controversial. In the present study, we investigated the effects of APN on CIA mice using APN-producing adenovirus.

Materials and methods

Materials. Enzyme-linked immunosorbent assay (ELISA) for murine APN (including all isoforms) was purchased from Otsuka Pharmaceutical (Tokyo, Japan). Anti-APN polyclonal antibody used

* Corresponding author. Fax: +81 6 6879 3739.
E-mail address: ichi@imed2.med.osaka-u.ac.jp (I. Shimomura).

0006-291X/$ - see front matter © 2008 Elsevier Inc. All rights reserved.
doi:10.1016/j.bbrc.2008.11.005

for Western blotting was described previously [6]. Tartrate-resistant acid phosphatase (TRAP) staining kit was purchased from Cell Garage (Tokyo, Japan).

Induction and assessment of CIA. To induce CIA, we injected intradermally 100 μl of an emulsion containing 200 μg of chicken CII (Sigma, St. Louis, MO) and 200 μg of *Mycobacterium tuberculosis* in CFA (Chondrex, Redmond, WA) at the base of the tail of 6-week-old male DBA/1J mice (CLEA Japan, Tokyo), twice with a 21-day gap, as described previously [7]. Clinical severity of arthritis was assessed as described previously [8]. Each limb was scored, yielding a maximum possible score of 16 per mouse. Serum was collected from the tail vein at each time point.

APN adenovirus and systemic delivery in vivo. Adenovirus producing the full-length mouse APN was prepared as described previously [9]. Then, 200 μl of 2×10^8 plaque-forming units of adiponectin-producing adenovirus (Ad-APN) or control β-galactosidase-expressing adenovirus (Ad-β-gal) were injected into the jugular vein, on 19 (before arthritis progression) or 27 (during arthritis progression) days after initial injection of CII.

Determination of IgG, IgG2a, and IgG1 titers against CII and serum complement C1q and C3 levels. The total IgG anti-collagen antibody titers against chicken CII were determined through ELISA kit (Chondrex). IgG1 and IgG2a anti-collagen antibody titers against chicken CII were determined as described previously, and expressed in optical density (OD) value [10]. Serum C1q and C3 levels were determined by ELISA as described previously [11].

Histological analysis. On day 35 after initial injection of CII, joints were harvested and fixed in phosphate-buffered 4% paraformaldehyde, decalcified in 14% ethylenediaminetetraacetic acid (EDTA), and embedded in paraffin. Joint sections were stained with Safranin O and hematoxylin/eosin, and then histologically scored for inflammation, cartilage damage, and pannus formation as described previously [12]. Immunostaining for mouse IgG, C1q, C3, neutrophils, CXC chemokine ligand (CXCL)12, and APN was performed on paraffin-embedded samples with goat anti-mouse IgG (Cappel), rat anti-mouse C1q (Hycult Biotechnology b.v., Uden, Netherlands), rat anti-mouse C3 (Hycult Biotechnology), rat-anti-mouse neutrophils, (Serotec, Oxford, UK), monoclonal antihuman/mouse CXCL12 antibody (R&D Systems Inc., Minneapolis, MN), and rabbit-anti-mouse APN (Otsuka Pharmaceutical), respectively. The other steps were performed according to the instructions provided on the labeling of Vectastain Elite ABC system (Vector Laboratories, Burlingame, CA). Scoring for IgG, C1q and C3 staining on the cartilage, and CXCL12 staining on the synovium was performed as described previously [13]. The average number of infiltrating neutrophils in the synovium was determined using a modified version of the published method [14].

Quantitative real-time PCR of joint samples. Total RNA was extracted by pulverizing the frozen individual fore paws with an RNA STAT-60 kit. The first-strand cDNA was synthesized using ThermoScript RT-PCR System (Invitrogen, San Diego, CA). Real-time polymerase chain reaction (PCR) was performed on a Light Cycler using the Fast Start DNA Master SYBR Green I (Roche Diagnostics, Indianapolis, IN). The sequences of primers were designed based on a previous report [13], and other primers are listed in Supplementary Table 1.

Lymph node cell proliferation assay. In vitro proliferation of draining lymph node (DLN) cells was examined by Cell Proliferation ELISA Bromodeoxyuridine (BrdU) kit (Roche) using a modified version of the published method [10].

Cytokine production by cultured splenocytes. Spleens were removed and cell suspensions (2×10^6 cells/well) were distributed to flat bottom 96-well plates. Spleen cells were cultured without or with either 50 μg/ml heat-denatured chicken CII (Sigma–Aldrich) or 5 μg/ml LPS from *Escherichia coli* (Sigma–Aldrich). After 48-h incubation, the supernatants were collected, and TNF-α and IL-1β levels were measured using ELISA kit (Quantikine Mouse ELISA kit, R&D Systems Inc.).

Skeletal morphology. Three-dimensional microcomputed tomography (3D-μCT) scan for ankle joints was undertaken and the trabecular bone area (percentage of bone volume [BV] per tissue volume [TV]) of distal tibia was measured using a composite X-ray analysis system (Shimadzu, SMX-100CT-SV, Kyoto, Japan).

Statistical analysis and ethical considerations. Data were expressed as means ± standard error of the mean. Differences between groups were examined for statistical significance using Chi-square test, Student's *t* test, or analysis of variance with Fisher's protected least significant difference test. A *P* value less than 0.05 denoted the presence of a statistically significant difference. The experimental protocol was approved by the Ethics Review Committee for Animal Experimentation of Osaka University School of Medicine.

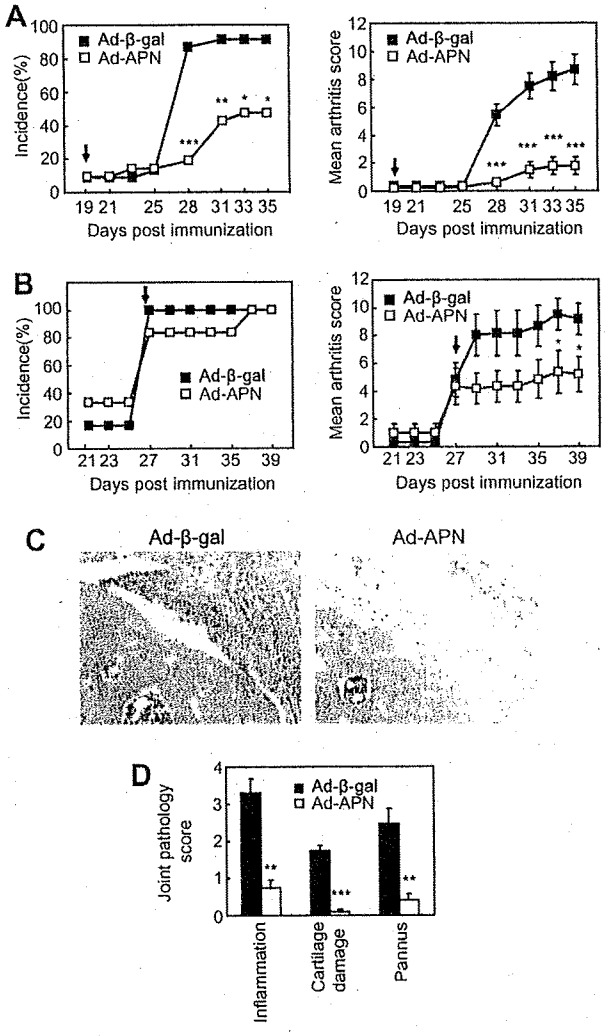

Fig. 1. Systemic delivery of APN in collagen-induced arthritis (CIA) mouse model and histological analysis of the joints. (A) On day 19, before arthritis progression, mice were injected with adenoviral vector directing the expression of either *lacZ* gene (Ad-β-gal) or APN (Ad-APN) intravenously ($n = 23$ Ad-β-gal-infected mice, $n = 21$ Ad-APN-infected mice). (B) On day 27, during arthritis progression, mice were injected with the same adenovirus ($n = 6$ mice in each group). (C) Histological features of representative hematoxylin and eosin-stained sections of the ankle joints (original magnification 200×), and (D) mean pathological scores of the joints of adenovirus-infected CIA mice ($n = 36$ joints in each group). $^{*}P < 0.05$, $^{**}P < 0.01$, $^{***}P < 0.001$, versus Ad-β-gal-infected CIA mice.

Results

Ad-APN suppresses progression of arthritis in CIA model

First, we tried two protocols to evaluate the effect of Ad-APN on CIA. When the virus was injected on day 19 (Fig. 1A), the incidence and disease activity on day 35 were significantly suppressed by Ad-APN treatment compared with Ad-β-gal (arthritis score: Ad-APN-infected mice: 1.76 ± 0.63, Ad-β-gal-infected mice: 8.68 ± 1.06; $P < 0.001$). In addition, when the virus was injected on day 27 (Fig. 1B), disease activity was significantly suppressed on day 39 by Ad-APN treatment compared with Ad-β-gal (arthritis score: Ad-APN-infected mice: 5.17 ± 1.25, Ad-β-gal-infected mice: 9.17 ± 1.15; $P < 0.05$). For the rest of this study, we used the former protocol (Fig. 1A). Histological analysis of the ankle joint showed typical features of active arthritis in Ad-β-gal-infected CIA mice, including infiltration of inflammatory cells into the synovium, cartilage damage, and pannus formation. These changes were significantly less pronounced in Ad-APN-infected CIA mice (Fig. 1C and D).

Ad-APN increases APN protein in serum and bone marrow, and does not alter serum anti-collagen antibodies or complement levels

In the experiments described in Fig. 1A, injection of Ad-APN resulted in about 5-fold increase on day 21 and about 30-fold increase on day 35 in serum APN levels (Fig. 2A). The high serum APN protein levels in Ad-APN-infected CIA mice were mainly composed of high- and middle-molecular weight forms of APN (Fig. 2B). Moreover, Ad-APN substantially increased APN protein content in knee joints compared with Ad-β-gal (Fig. 2C). Immunohistochemical staining of knee joints with anti-APN antibody indicated accumulation of APN in the bone marrow but not on the cartilage surface in Ad-APN-infected CIA mice (Fig. 2D). Under such conditions, anti-CII IgG, IgG2a, and IgG1 titers, serum C1q and C3 levels were not different between Ad-APN- and Ad-β-gal-infected CIA mice (Fig. 2E and F).

Treatment of CIA mice with Ad-APN suppresses local deposition of C1q and C3, infiltration of neutrophil, and changes in mRNAs of pro-inflammatory genes

Next, we examined the accumulation of IgG, C1q, and C3 on the cartilage of wrist, knee, and ankle joints by immunohistochemical staining (Fig. 3A and B). Under the conditions with minimum background staining, IgG deposition on the cartilage was observed in both adenovirus-infected CIA mice. On the other hand, C1q and C3 deposits on the cartilage were significantly suppressed by Ad-APN treatment compared with Ad-β-gal. Furthermore, neutrophil infiltration and synovium deposition of CXCL12, a chemokine that promotes leukocyte migration, were also significantly decreased in Ad-APN-infected CIA mice (Fig. 3A and B). To assess the inflammatory status, mRNA levels of pro-inflammatory genes, complement factors, and F4/80 (a marker of monocyte/macrophage linage) were measured in isolated forepaws. The expression levels of IL-1β, IL-6, COX-2 IFN-γ, TNF-α, C1q, C3, and F4/80 were all significantly decreased by Ad-APN treatment (Fig. 3C).

Effects of Ad-APN on immunocyte activities in lymph nodes and spleen, and bone erosion of CIA mice

Next, activities of immunocytes were measured. DLN cells from Ad-APN-infected CIA mice showed marginally inhibited proliferation activities (Fig. 4A). Splenocytes from Ad-APN-infected CIA

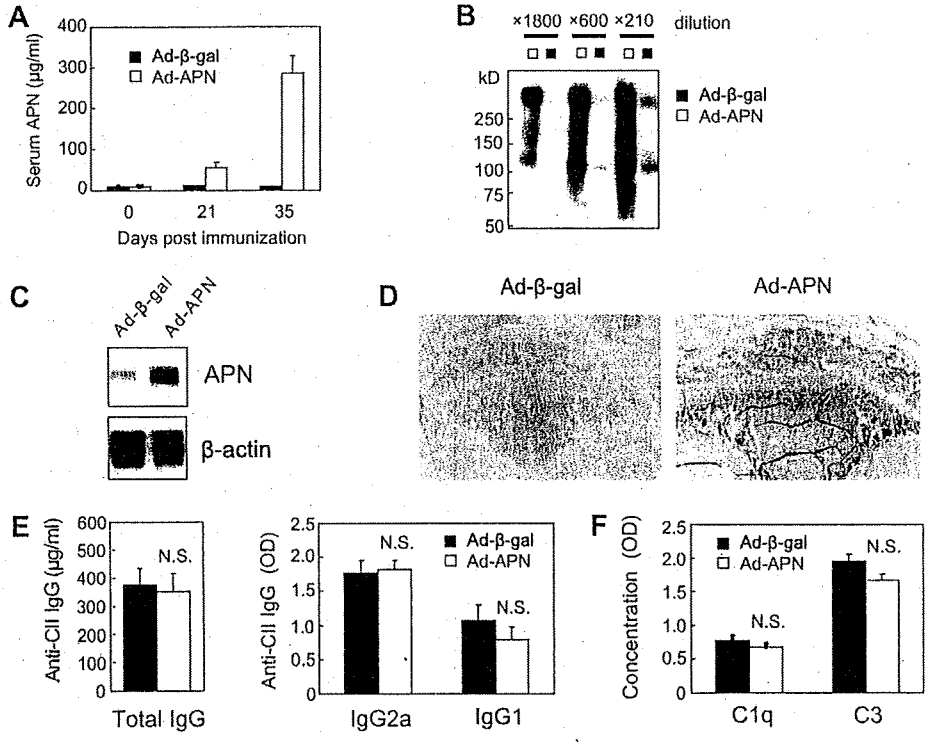

Fig. 2. High APN levels in serum and joints do not alter serum levels of anti-CII antibody, complement C1q, or C3 in CIA mice. (A) Serum APN concentrations at each time point were determined by ELISA ($n = 6$ in each group). Representative serum samples (B) and protein lysates prepared from knee joints (C) of adenovirus-infected CIA mice on day 35 were subjected sodium dodecyl sulfate-polyacrylamide gel electrophoresis without reducing reagent, and analyzed by western blot using anti-APN antibody. (D) Representative sections of proximal tibia immunostained with APN (original magnification 40×). Serum samples were obtained on day 35, and anti-CII specific IgG, IgG2a, and IgG1 levels (E), and complement C1q and C3 levels (F) were measured by ELISA ($n = 6$ in each group). NS = not significant.

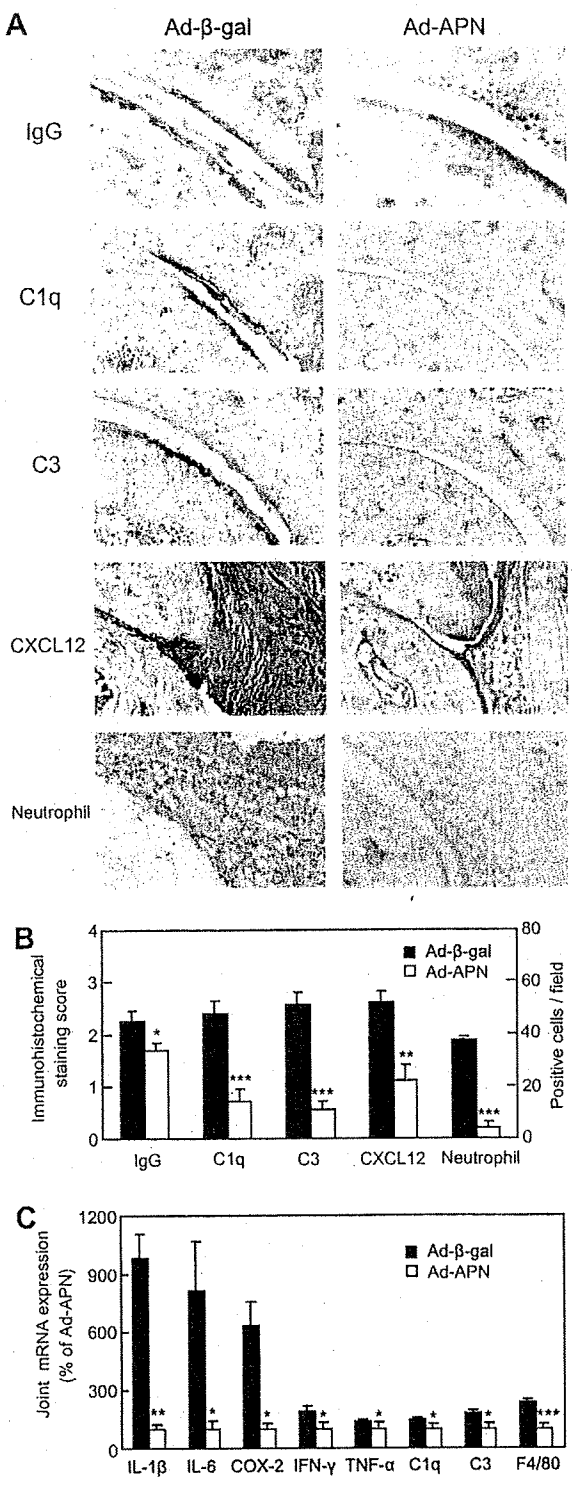

Fig. 3. Ad-APN inhibits complement deposition/expression and pro-inflammatory cytokine/enzyme expression in CIA mice. (A) Representative sections immunostained for IgG, C1q, C3, CXCL12, and neutrophil on the cartilage surface and synovium of the ankle joints of adenovirus-infected CIA mice (original magnification 200×). (B) Scoring of immunostained joint sections from adenovirus-infected CIA mice ($n = 16$ joints in each group). (C) mRNA expression levels in forepaws of adenovirus-infected CIA mice. ($n = 6$ joints in each group). Values are normalized to the level of 36B4 mRNA. $^{*}P < 0.05$, $^{**}P < 0.01$, $^{***}P < 0.001$, versus Ad-β-gal-infected CIA mice.

mice produced less IL-1β in all conditions, and less TNF-α in response to LPS *in vitro* (Fig. 4B). Finally, analysis of bone erosion of the distal tibia using μCT revealed that trabecular bone volume were significantly decreased in Ad-β-gal-infected CIA mice compared to those in Ad-APN-infected CIA mice (Fig. 4C). In addition, the number of TRAP-positive cells was significantly decreased in ankle joints of Ad-APN-infected CIA mice (Fig. 4D).

Discussion

In the present study, we demonstrated for the first time that Ad-APN significantly improved joint inflammation and bone erosion in CIA mice. There were no significant differences in anti-CII IgG, C1q, and C3 levels between Ad-APN and Ad-β-gal infected CIA mice (Fig. 2E and F), indicating that Ad-APN has little effect on humoral immunity. On the other hand, C1q and C3 deposition were markedly suppressed on the cartilage surface of Ad-APN-infected CIA mice (Fig. 3A and B). Therefore, we investigated the direct effect of APN on complement activation. APN has a substantial sequence similarity to C1q, and also binds to C1q receptor [15]. In addition, we confirmed the binding between human recombinant APN from mammalian cells and human C1q *in vitro* as reported previously [16]. However, in our preliminary experiments, this recombinant APN did not alter C1q binding to adherent CII-IC [11], CII-IC-induced mouse serum C3 activation (mainly involves classical pathway) [11], or zymosan-induced mouse serum C3 activation (mainly involves alternative pathway) [10] *in vitro* (data not shown). To elucidate the direct effect of APN on the complement activation, further *in vivo* and *in vitro* analyses are required.

We showed marked suppression of C1q and C3 deposition, accompanied by significant downregulation of C1q, C3, and F4/80 mRNAs in the Ad-APN-infected CIA joints (Fig. 3). A previous report demonstrated that APN inhibited the expression of endothelial adhesion molecules induced by TNF-α, and consequent transendothelial migration of monocytes [17]. In addition, TNF-α-induced vascular permeability is required for the migration of inflammatory cells into the joint and development of inflammatory process in mouse arthritis models [1], and APN was reported to inhibit TNF-α-induced hyperpermeability in endothelial cells [18]. Our group demonstrated that APN was protective against murine colitis through inhibition of macrophages infiltration and release of pro-inflammatory cytokines [19]. Considering that C1q is mainly produced by monocyte/macrophage linage [20], and C3 is produced by liver and inflamed synoviocytes [21], reduced accumulation of F4/80 positive cells and consequent C3 production by inflamed synovium should result in suppression of complement deposition and pro-inflammatory cytokine production in the CIA joints.

We also observed that Ad-APN suppressed synovial deposition of CXCL12. CXCL12 is a chemokine anchored to heparan sulfate (HS) proteoglycans on endothelial cells of RA synovium [22], and acts as a critical chemoattractant in the pathogenesis of CIA [23]. APN inhibits the binding of CXCL12 to HS, and alters the distribution of CXCL12 at the site of inflammation [24]. Taken together, Ad-APN may improve joint inflammation through decreased CXCL12 deposition in CIA synovium.

Previous studies showed that the cellular immunity, represented by the activity of immunocytes of lymph nodes or spleen, is causally associated with the disease activity in CIA mice [25]. In this study, Ad-APN marginally reduced DLN cells proliferation (Fig. 4A), and significantly suppressed IL-1β production and TNF-α production from splenocytes (Fig. 4B). These results indicate that Ad-APN could suppress disease activity of CIA partially through inhibition of cellular immunity.

In this study, Ad-APN reduced the number of TRAP-positive cells and resulted in amelioration of bone erosion in the joints of CIA mice (Fig. 4C and D). Previously, we and others reported that

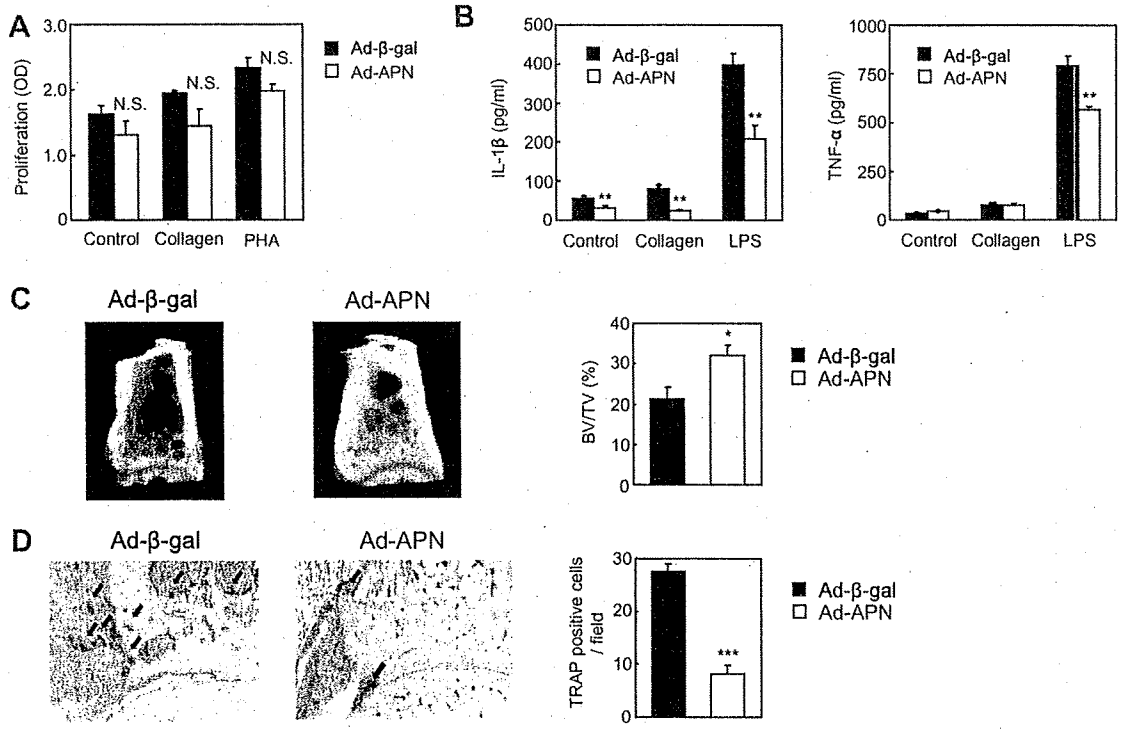

Fig. 4. Effects of Ad-APN on DLN cell proliferation and pro-inflammatory cytokine production from splenocytes, and bone erosion in CIA. All samples were obtained on day 35. (A) Proliferative response of DLN cells obtained from adenovirus-infected CIA mice. Isolated cells from lymph nodes were cultured for 72 h without (control) or with either 50 μg/ml heat-denatured chicken CII or 5 μg/ml phytohemagglutinin (PHA). (B) Production of pro-inflammatory cytokine by splenocytes from adenovirus-infected CIA mice. IL-1β and TNF-α levels were measured in supernatants of splenocytes by specific ELISA. (C) Three-dimensional μCT scan of the distal tibia of adenovirus-infected CIA mice. Trabecular bone volume is expressed as percentage of total tissue volume (BV/TV [%]) ($n = 4$ joints in each group). (D) Reduced number of osteoclasts in Ad-APN-infected CIA mice joints. Sections of ankle joints stained with TRAP (original magnification 100×). The number of TRAP-positive cells was counted in 5 randomly selected fields ($n = 8$ joints in each group). NS = not significant, $^{*}P < 0.05$, $^{**}P < 0.01$, $^{***}P < 0.001$, versus Ad-β-gal-infected CIA mice.

APN inhibits osteoclasts differentiation in RAW264 cells [26] and mouse bone marrow macrophages [9]. Collectively, besides anti-inflammatory effects in the joints, Ad-APN might directly inhibits bone erosion of CIA mice by inhibiting osteoclasts differentiation.

The present study demonstrates for the first time that systemic APN delivery provides protection against the development of inflammatory arthritis in a murine model, through several anti-inflammatory mechanisms. The results provide new insights on the role of APN in inflammatory arthritis and new strategies for the treatment.

Acknowledgments

We are grateful to Dr. T. Maeda for great help with the experiments. We also thank M. Shinkawa and F. Katsube for the excellent support in tissue processing for histological analysis. This work was supported by grants from the Ministry of Health, Labour, and Welfare of Japan.

Appendix A. Supplementary data

Supplementary data associated with this article can be found, in the online version, at doi:10.1016/j.bbrc.2008.11.005.

References

[1] J.A. Luross, N.A. Williams, The genetic and immunopathological processes underlying collagen-induced arthritis, Immunology 103 (2001) 407–416.
[2] P.E. Scherer, S. Williams, M. Fogliano, G. Baldini, H.F. Lodish, A novel serum protein similar to C1q, produced exclusively in adipocytes, J. Biol. Chem. 270 (1995) 26746–26749.
[3] M.C. Wulster-Radcliffe, K.M. Ajuwon, J. Wang, J.A. Christian, M.E. Spurlock, Adiponectin differentially regulates cytokines in porcine macrophages, Biochem. Biophys. Res. Commun. 316 (2004) 924–929.
[4] L. Senolt, K. Pavelka, D. Housa, M. Haluzik, Increased adiponectin is negatively linked to the local inflammatory process in patients with rheumatoid arthritis, Cytokine 35 (2006) 247–252.
[5] C.H. Tang, Y.C. Chiu, T.W. Tan, R.S. Yang, W.M. Fu, Adiponectin enhances IL-6 production in human synovial fibroblast via an AdipoR1 receptor, AMPK, p38, and NF-kappa B pathway, J. Immunol. 179 (2007) 5483–5492.
[6] N. Maeda, M. Takahashi, T. Funahashi, S. Kihara, H. Nishizawa, K. Kishida, H. Nagaretani, M. Matsuda, R. Komuro, N. Ouchi, H. Kuriyama, K. Hotta, T. Nakamura, I. Shimomura, Y. Matsuzawa, PPARgamma ligands increase expression and plasma concentrations of adiponectin, an adipose-derived protein, Diabetes 50 (2001) 2094–2099.
[7] S. Nakae, A. Nambu, K. Sudo, Y. Iwakura, Suppression of immune induction of collagen-induced arthritis in IL-17-deficient mice, J. Immunol. 171 (2003) 6173–6177.
[8] E. Gonzalez-Rey, A. Chorny, N. Varela, F. O'Valle, M. Delgado, Therapeutic effect of urocortin on collagen-induced arthritis by down-regulation of inflammatory and Th1 responses and induction of regulatory T cells, Arthritis Rheum. 56 (2007) 531–543.
[9] K. Oshima, A. Nampei, M. Matsuda, M. Iwaki, A. Fukuhara, J. Hashimoto, H. Yoshikawa, I. Shimomura, Adiponectin increases bone mass by suppressing osteoclast and activating osteoblast, Biochem. Biophys. Res. Commun. 331 (2005) 520–526.
[10] N.K. Banda, D. Kraus, A. Vondracek, L.H. Huynh, A. Bendele, V.M. Holers, W.P. Arend, Mechanisms of effects of complement inhibition in murine collagen-induced arthritis, Arthritis Rheum. 46 (2002) 3065–3075.
[11] N.K. Banda, K. Takahashi, A.K. Wood, V.M. Holers, W.P. Arend, Pathogenic complement activation in collagen antibody-induced arthritis in mice requires amplification by the alternative pathway, J. Immunol. 179 (2007) 4101–4109.
[12] A. Bendele, T. McAbee, G. Sennello, J. Frazier, E. Chlipala, D. McCabe, Efficacy of sustained blood levels of interleukin-1 receptor antagonist in animal models of arthritis: comparison of efficacy in animal models with human clinical data, Arthritis Rheum. 42 (1999) 498–506.
[13] N.K. Banda, J.M. Thurman, D. Kraus, A. Wood, M.C. Carroll, W.P. Arend, V.M. Holers, Alternative complement pathway activation is essential for inflammation and joint destruction in the passive transfer model of collagen-induced arthritis, J. Immunol. 177 (2006) 1904–1912.

[14] Z. Liu, X. Xu, H.C. Hsu, A. Tousson, P.A. Yang, Q. Wu, C. Liu, S. Yu, H.G. Zhang, J.D. Mountz, CII-DC-AdTRAIL cell gene therapy inhibits infiltration of CII-reactive T cells and CII-induced arthritis, J. Clin. Invest. 112 (2003) 1332–1341.
[15] T. Yokota, K. Oritani, I. Takahashi, J. Ishikawa, A. Matsuyama, N. Ouchi, S. Kihara, T. Funahashi, A.J. Tenner, Y. Tomiyama, Y. Matsuzawa, Adiponectin, a new member of the family of soluble defense collagens, negatively regulates the growth of myelomonocytic progenitors and the functions of macrophages, Blood 96 (2000) 1723–1732.
[16] P.W. Peake, Y. Shen, A. Walther, J.A. Charlesworth, Adiponectin binds C1q and activates the classical pathway of complement, Biochem. Biophys. Res. Commun. 367 (2008) 560–565.
[17] N. Ouchi, S. Kihara, Y. Arita, K. Maeda, H. Kuriyama, Y. Okamoto, K. Hotta, M. Nishida, M. Takahashi, T. Nakamura, S. Yamashita, T. Funahashi, Y. Matsuzawa, Novel modulator for endothelial adhesion molecules: adipocyte-derived plasma protein adiponectin, Circulation 100 (1999) 2473–2476.
[18] S.Q. Xu, K. Mahadev, X. Wu, L. Fuchsel, S. Donnelly, R.G. Scalia, B.J. Goldstein, Adiponectin protects against angiotensin ii or tumor necrosis factor {alpha}-induced endothelial cell monolayer hyperpermeability. Role of cAMP/PKA signaling, Arterioscler Thromb. Vasc. Biol. (2008).
[19] T. Nishihara, M. Matsuda, H. Araki, K. Oshima, S. Kihara, T. Funahashi, I. Shimomura, Effect of adiponectin on murine colitis induced by dextran sulfate sodium, Gastroenterology 131 (2006) 853–861.
[20] Y. Takemura, N. Ouchi, R. Shibata, T. Aprahamian, M.T. Kirber, R.S. Summer, S. Kihara, K. Walsh, Adiponectin modulates inflammatory reactions via calreticulin receptor-dependent clearance of early apoptotic bodies, J. Clin. Invest. 117 (2007) 375–386.
[21] P.A. Monach, A. Verschoor, J.P. Jacobs, M.C. Carroll, A.J. Wagers, C. Benoist, D. Mathis, Circulating C3 is necessary and sufficient for induction of autoantibody-mediated arthritis in a mouse model, Arthritis Rheum. 56 (2007) 2968–2974.
[22] J.L. Pablos, B. Santiago, M. Galindo, C. Torres, M.T. Brehmer, F.J. Blanco, F.J. Garcia-Lazaro, Synoviocyte-derived CXCL12 is displayed on endothelium and induces angiogenesis in rheumatoid arthritis, J. Immunol. 170 (2003) 2147–2152.
[23] B. De Klerck, L. Geboes, S. Hatse, H. Kelchtermans, Y. Meyvis, K. Vermeire, G. Bridger, A. Billiau, D. Schols, P. Matthys, Pro-inflammatory properties of stromal cell-derived factor-1 (CXCL12) in collagen-induced arthritis, Arthritis Res. Ther. 7 (2005) R1208–1220.
[24] H. Masaie, K. Oritani, T. Yokota, I. Takahashi, T. Shirogane, H. Ujiie, M. Ichii, N. Saitoh, T. Maeda, R. Tanigawa, K. Oka, Y. Hoshida, Y. Tomiyama, Y. Kanakura, Adiponectin binds to chemokines via the globular head and modulates interactions between chemokines and heparan sulfates, Exp. Hematol. 35 (2007) 947–956.
[25] N.K. Banda, A. Vondracek, D. Kraus, C.A. Dinarello, S.H. Kim, A. Bendele, G. Senaldi, W.P. Arend, Mechanisms of inhibition of collagen-induced arthritis by murine IL-18 binding protein, J. Immunol. 170 (2003) 2100–2105.
[26] N. Yamaguchi, T. Kukita, Y.J. Li, N. Kamio, S. Fukumoto, K. Nonaka, Y. Ninomiya, S. Hanazawa, Y. Yamashita, Adiponectin inhibits induction of TNF-alpha/RANKL-stimulated NFATc1 via the AMPK signaling, FEBS Lett. 582 (2008) 451–456.

Clin Rheumatol (2009) 28:445–451
DOI 10.1007/s10067-008-1074-y

ORIGINAL ARTICLE

Serum adiponectin concentrations correlate with severity of rheumatoid arthritis evaluated by extent of joint destruction

Kosuke Ebina · Atsunori Fukuhara · Wataru Ando · Makoto Hirao · Tadashi Koga · Kazuya Oshima · Morihiro Matsuda · Kazuhisa Maeda · Tadashi Nakamura · Takahiro Ochi · Iichiro Shimomura · Hideki Yoshikawa · Jun Hashimoto

Received: 12 October 2008 / Revised: 30 November 2008 / Accepted: 3 December 2008 / Published online: 16 December 2008

Abstract Adiponectin is a hormone released by adipose tissue with antidiabetic, antiatherogenic, and anti-inflammatory properties. The present observational study focused on the relation between serum adiponectin level and the disease severity of established rheumatoid arthritis (RA). Ninety patients with more than 5-year diagnosis of RA and 42 age- and BMI-matched control were enrolled. The severity of RA was evaluated according to the number of destructed joints of overall 68 joints on plain radiographs (37 patients had mild RA and 53 had severe RA). Serum adiponectin level was significantly higher in the severe RA group (17.7±6.7 μg/ml) than in the control (9.1±3.8 μg/ml) and mild RA groups (13.9±6.5 μg/ml) (control vs. mild RA group, $P<0.001$; mild RA vs. severe RA group, $P<0.01$). These results suggest that increased number of joint destruction is associated with hyperadiponectinemia in established RA patients.

Keywords Adiponectin · Disease severity · Number of joint destruction · Rheumatoid arthritis

Introduction

Adiponectin is a hormone released by adipose tissue and has various biological properties, such as antidiabetic [1], antiatherogenic [2], and anti-inflammatory effects [3]. Part

K. Ebina · W. Ando · M. Hirao · K. Oshima · H. Yoshikawa · J. Hashimoto (✉)
Department of Orthopaedics, Graduate School of Medicine, Osaka University, 2-2 Yamadaoka, Suita, Osaka 565-0871, Japan
e-mail: junha@ort.med.osaka-u.ac.jp

K. Ebina · A. Fukuhara · M. Matsuda · K. Maeda · T. Nakamura · I. Shimomura
Department of Metabolic Medicine, Graduate School of Medicine, Osaka University, 2-2 Yamadaoka, Suita, Osaka 565-0871, Japan

T. Koga
Biometrics Department, Shin Nippon Biomedical Laboratories, Ltd, 2438 Miyanoura, Kagoshima, Kagoshima 891-1394, Japan

M. Matsuda
Division of Analysis for Pathophysiology, Institute of Clinical Research, National Hospital Organization Kure Medical Center, Kure, Hiroshima 737-0023, Japan

M. Matsuda
Department of Internal Medicine, National Hospital Organization Kure Medical Center, Kure, Hiroshima 737-0023, Japan

T. Ochi
Osaka Police Hospital, 10-31 Kitayama-cho, Tennoji-ku, Osaka 543-0035, Japan

of these effects is mediated by suppressing the production of tumor necrosis factor (TNF)-α and interleukin (IL)-6 by activated macrophage [3]. In addition, it has been reported that adiponectin stimulates the proliferation and differentiation of human osteoblasts [4] and suppresses the differentiation of osteoclasts [5], suggesting that adiponectin may play a role in rheumatoid arthritis (RA).

A recent clinical study showed that serum adiponectin concentrations are higher in RA patients than in healthy control [6, 7]. In addition, adiponectin induces the production of pro-inflammatory IL-6 from RA synovial fibroblasts in vitro [8], suggesting that adiponectin is a potent driving force of arthritis. On the other hand, another report demonstrated that adiponectin concentrations correlated negatively with the number of leukocytes in the synovial fluid of RA patients [7], indicating that adiponectin is a counterpart of the local inflammatory process. Thus, the role of adiponectin in RA is controversial. In a step to define the role of adiponectin in RA, the present study was designed to investigate the correlation between serum adiponectin level and RA disease severity.

Materials and methods

Patients

We have previously reported that serum adiponectin level is significantly higher in females than in males and negatively correlates with body mass index (BMI) [9]. In addition, previous reports have demonstrated that most of the progression of joint damage in RA occurs during the first years of the disease and decreases thereafter [10, 11]. Therefore, to investigate the correlation between serum adiponectin level and disease severity and joint destruction in established RA, 90 female patients with more than 5-year history of RA were enrolled in this study. RA was diagnosed based on the 1987 revised American College of Rheumatology (ACR) criteria [12]. The first assessment was carried out from September to November, 2005, and 18 patients were enrolled in the second assessment from March to April, 2008, about 2.5 years after the first assessment. Sixty-five patients (72.2%) were treated with oral prednisolone and 48 patients (53.3%) with methotrexate. All patients were followed-up at Osaka University Hospital.

For non-RA controls, 42 age- and BMI-matched women who underwent health examination at the institutions that participated in the Japanese Visceral Fat Syndrome (J-VFS) Study Committee of the Ministry of Health and Welfare of Japan and subjects who visited Osaka University Hospital for health check were enrolled in the present study [13]. Patients treated with antihypertensive, antidiabetic, or antihyperlipidemic regimen or patients who met the definition of each disease indicated in the relevant guidelines were defined as having hypertension, diabetes, and hyperlipidemia, respectively. Patients treated with drugs influencing serum adiponectin levels, such as anti-TNF-α [14, 15], insulin [16], thiazolidinediones [17], telmisartan [18], glimepiride [19], and all other biologics were excluded in this study. The study was approved by the Ethical Committee of Osaka University School of Medicine and written informed consent was obtained from each patient.

Assessment of disease severity and disease activity

The severity of RA was evaluated by the number of joints with erosions among 68 joints of whole body using plain radiographs, as described previously [20]. Joint erosion was defined as changes equal to or more severe than stage II according to the criteria of Steinbocker et al. [21]. Patients were classified according to disease severity as described previously [22]. Briefly, the least erosive subset (LES) group exhibited erosions in less than 20 joints and erosive articular changes limited to the small peripheral joints of hands or feet. The more erosive subset (MES) group had erosions in more than 21 joints and erosive articular changes in large axial joints. The most erosive subset with mutilating disease (MUD) group, that had erosions in more than 46 joints, and almost all joints were extensively damaged in the early period of RA. In this study, we categorized LES patients as the "mild RA group" (n=37), and MES/MUD patients as the "severe RA group" (n=53). Disease activity score including a 28 joint count/CRP (DAS28-CRP) was evaluated as described previously [23].

Measurement of serum adiponectin concentrations

Total serum adiponectin level (including all isoforms) was measured with an enzyme-linked immunosorbent assay (ELISA) kit (Otsuka Pharmaceutical, Tokyo, Japan), as reported previously [13].

Statistical analysis

Data are expressed as mean ± standard deviation (SD). Differences in variables between the mild and severe RA groups were assessed by the Mann–Whitney U test and the chi-square test. Changes in serum adiponectin levels between the first and second assessment was examined by the Wilcoxon's signed rank test. The influence of serum adiponectin level on other variables was investigated by calculating Spearman's correlation coefficients. The correlation between BMI and disease severity was investigated by logistic regression analysis. Conditional multivariate logistic regression models were constructed and odds ratios (ORs) and 95% confidence intervals (95% CI) were cal-

culated to investigate the association of serum adiponectin level on disease severity, with adjustment for BMI. To investigate the cutoff value for serum adiponectin, a value yielding 80% correspondence to the severity of RA was estimated by a logistic regression model and statistical significance was estimated by Fisher's exact test. Probability values of less than 0.05 were considered statistically significant. All statistical analyses were carried out with SAS software version 9.1.3 (SAS Institute, Cary, NC, USA).

Results

Clinical and biochemical characteristics of the study subjects

There were no significant differences between mild and severe RA groups in age (60.8±11.0 vs. 61.7±11.7 years), disease duration (15.5±6.9 vs. 17.3±6.8 years), body mass index (22.1±3.4 vs. 20.8±3.0 kg/m^2), and prevalence of hypertension (18.8% vs. 28.3%), diabetes (16.2 vs. 18.9%), and hyperlipidemia (21.6 vs. 24.5%). The age and BMI of subjects of the control group were 61.0±11.4 years and 21.9±3.2 kg/m^2, respectively. The prevalence of each

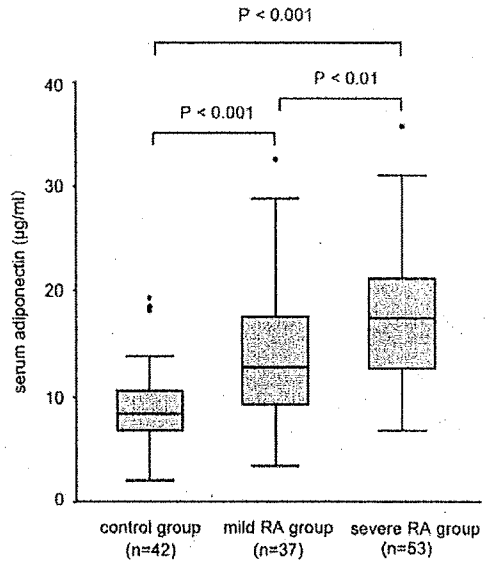

Fig. 1 Box-and-whisker plots of serum adiponectin levels in the control group, mild RA group, and severe RA group evaluated by the number of joint destruction in 68 joints on plain radiograph. The mean serum level of adiponectin was significantly higher in the severe RA group (17.7±6.7 μg/ml) than in the control (9.1±3.8 μg/ml) or mild RA group (13.9±6.5 μg/ml) (control vs. mild RA group: $P<0.001$, mild RA vs. severe RA group: $P<0.01$, control vs. severe RA group: $P<0.001$)

Table 1 Baseline demographic, laboratory, and clinical characteristics of the two RA groups

	mild RA group (n=37)	severe RA group (n=53)	P[a] value
Age, years	60.8±11.0	61.7±11.7	NS
Duration of disease, years	15.5±6.9	17.3±6.8	NS
Body mass index, kg/m^2	22.1±3.4	20.8±3.0	NS
CRP, mg/l	0.9±1.3	1.9±2.0	0.003
MMP-3, ng/ml	146.5±150.9	222.8±177.6	0.047
IL-6, pg/ml	14.5±36.0	18.1±26.2	NS
RF titer, IU/ml	158.1±417.0	235.7±366.9	NS
RF positivity, % patients	77.1%	82.7%	NS[b]
BAP, U/l	24.0±13.5	23.9±9.5	NS
iOC, ng/ml	6.9±3.5	6.7±7.3	NS
1CTP, ng/ml	4.9±1.9	6.5±3.1	0.010
uDPD, nmol/mmol creatinine	6.6±2.2	7.9±3.2	NS
DAS28-CRP	2.2±1.0	3.1±1.5	0.001
Prednisolone dosage, mg/day	2.2±2.5	4.3±3.6	0.001
Methotrexate dosage, mg/week	4.3±3.2	4.4±3.6	NS
Adiponectin, μg/ml	13.9±6.5	17.7±6.7	0.008

Data are mean ± SD

RA rheumatoid arthritis, *NS* not significant, *CRP* C-reactive protein, *MMP-3* matrix metalloproteinase-3, *IL-6* interleukin-6, *RF* rheumatoid factor, *BAP* bone-specific alkaline phosphatase, *iOC* intact osteocalcin, *1CTP* pyridinoline cross-linked carboxyterminal telopeptide of type 1 collagen, *uDPD* urinary deoxypyridinoline, *DAS28-CRP* disease activity score including a 28-joint count/CRP

[a] Except where otherwise indicated, determined by Mann–Whitney U test

[b] Except where otherwise indicated, determined by chi-square test

Table 2 Spearman's correlation analysis of the relation between serum adiponectin and other variables in all RA patients

Variable	r value	P value
Age, years	0.046	NS
Duration of disease, years	0.068	NS
Body mass index, kg/m^2	−0.269	0.011
CRP, mg/liter	0.078	NS
MMP-3, ng/ml	0.098	NS
IL-6, pg/ml	0.120	NS
RF titer, IU/ml	−0.033	NS
BAP, U/l	−0.193	NS
iOC, ng/ml	−0.075	NS
1CTP, ng/ml	0.033	NS
uDPD, nmol/mmol creatinine	−0.002	NS
DAS28-CRP	0.096	NS
Prednisolone dosage, mg/day	0.040	NS

r value Spearman's rank correlation coefficient, *NS* not significant, *CRP* C-reactive protein, *MMP-3* matrix metalloproteinase-3, *IL-6* interleukin-6, *RF* rheumatoid factor, *BAP* bone-specific alkaline phosphatase, *iOC* intact osteocalcin, *1CTP* pyridinoline cross-linked carboxyterminal telopeptide of type 1 collagen, *uDPD* urinary deoxypyridinoline, *DAS28-CRP* disease activity score including a 28-joint count/CRP

Table 3 Results of Spearman's rank correlation analysis of the relation between adiponectin and other variables with a significant difference between the severe and mild RA groups

	CRP	MMP-3	1CTP	DAS28-CRP	Prednisolone	Adiponectin
CRP		0.574***	0.486***	0.717***	0.335**	0.078
MMP-3			0.331**	0.532***	0.510***	0.098
1CTP				0.389***	0.220*	0.033
DAS28-CRP					0.372**	0.096
Prednisolone						0.040

CRP C-reactive protein, *MMP-3* matrix metalloproteinase-3, *1CTP* pyridinoline cross-linked carboxyterminal telopeptide of type 1 collagen, *DAS28-CRP* disease activity score including a 28-joint count/CRP
*$P<0.05$; **$P<0.01$; ***$P<0.001$

disease in the control group was 0% for hypertension, 2.3% for diabetes, and 9.5% for hyperlipidemia. Patients of the severe RA group had a significantly higher serum C-reactive protein (CRP) ($P=0.003$), matrix metalloproteinase (MMP)-3 ($P=0.047$), pyridinoline cross-linked carboxyterminal telopeptide of type 1 collagen (1CTP) ($P=0.010$), disease activity score including a 28-joint count/CRP (DAS28-CRP) ($P=0.001$), and prednisolone dose ($P=0.001$) than the mild RA group (Table 1), reflecting high inflammatory state and bone resorption level in this group as described previously [24]. The mean serum level of adiponectin was significantly higher in the total RA group (16.1±6.8 μg/ml) than in the control group (9.1±3.8 μg/ml) ($P<0.001$). Moreover, the mean serum level of adiponectin was significantly higher in the severe RA group (17.7±6.7 μg/ml) than in the control (9.1±3.8 μg/ml) or mild RA group (13.9±6.5 μg/ml) (control vs. mild RA group, $P<0.001$; mild RA vs. severe RA group, $P<0.01$, control vs. severe RA group, $P<0.001$) (Fig. 1). Univariate analysis of the relationship between serum adiponectin level and other variables showed that adiponectin correlated negatively with BMI ($r=-0.269$, $P=0.011$), but did not correlate with other variables such as inflammatory markers, bone metabolism markers, DAS28-CRP, or the dose of prednisolone (Table 2). Calculation of Spearman's rank correlation coefficients for the variables with a significant difference between the mild and severe RA groups showed that CRP correlated with MMP-3 ($r=0.574$, $P<0.001$), 1CTP ($r=0.486$, $P<0.001$), DAS28-CRP($r=0.717$, $P<0.001$), and dose of prednisolone ($r=0.335$, $P<0.01$), while there was no significant correlation with adiponectin ($r=0.078$, $P>0.05$) (Table 3). In addition, the dose of prednisolone correlated with CRP, MMP-3, 1CTP, and DAS28-CRP, but not with adiponectin ($r=0.040$, $P>0.05$) (Table 3). Multivariate logistic regression analyses revealed that even when the odds ratios were adjusted for BMI, serum adiponectin level significantly correlates with disease severity of RA ($P=0.031$) (Table 4).

Cutoff point of serum adiponectin for severe RA

Figure 2 shows the histogram of serum adiponectin levels of patients of the mild and severe RA groups. For clinical translation, the cutoff levels were selected. The cutoff value for serum adiponectin level was estimated at 18 μg/ml, yielding 80% correspondence with the severity of RA. Among the patients with serum adiponectin level of ≥18 μg/ml, 81.3% (26/32) belonged to the severe RA group and 18.8% (6/32) belonged to the mild RA group. This cutoff line showed significant correlation with disease severity ($P<0.01$). The specificity of this cutoff value was 53.4% (31/58) (Table 5).

Changes in serum adiponectin levels and severity of RA during follow-up

To further investigate the time-course changes of serum adiponectin levels and severity of RA, 18 patients underwent a second assessment 2.5 years later (Fig. 3). The mean serum adiponectin level of all patients did not change significantly, although it showed tendency to increase (14.0±5.5 to 15.2±5.2 μg/ml; $P=0.07$). Furthermore, the mean serum adiponectin level did not change significantly within the RA group (10.8±5.8 to 12.4±5.8 μg/ml in the mild RA group, $P=0.122$ and 17.2±2.7 to 18.0±2.4 μg/ml in the severe RA group, $P=0.372$). Assessment of RA severity revealed that none of the mild RA patients progressed to severe RA (data not shown).

Table 4 Adjusted ORs of serum adiponectin level and BMI for disease severity of RA

	Adjusted OR	95% CI	*P* value
Adiponectin, μg/ml	1.085	1.007–1.168	0.031
BMI, kg/m^2	0.907	0.785–1.048	NS

ORs odds ratios, *95% CI* 95% confidence interval, *NS* not significant

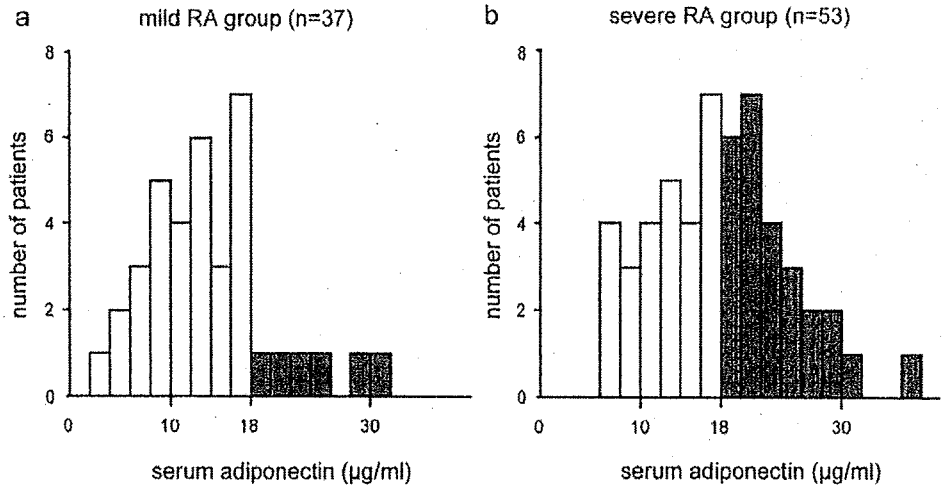

Fig. 2 Histograms showing the distribution of serum adiponectin levels in mild RA group (a) and severe RA group (b). Each column covers a serum adiponectin range of 2 μg/ml. When the cutoff value for adiponectin was set at 18 μg/ml, there was 80% correspondence with the severity of RA. Among patients with serum adiponectin levels ≥18 μg/ml, 81.3% (26/32) belonged to the severe RA group and 18.8% (6/32) belonged to the mild RA group

Discussion

The long-term functional prognosis of RA patients in daily life is mainly determined by the extent of damage in large joints such as the hip, knee, ankle, subtalar, shoulder, and elbow joints, rather than in small joints of the hands or feet. A previous report using Ochi's method demonstrated that MES and MUD groups underwent higher frequency of total knee or hip replacement than LES group (54.7% vs. 0.5%) [25], suggesting that Ochi's method offers some advantages for assessing large joint destruction [20, 25–27]. Therefore, we used Ochi's method to evaluate the severity of RA, to investigate the factors associated with the extent of overall joint destruction, especially in large joints [20]. Evaluation using this method revealed that markers associated with RA activity, such as CRP, MMP-3, 1CTP, and DAS28-CRP were all significantly higher in the severe RA group than in the mild RA group. These results were in agreement with previously published reports evaluated by the modified Sharp/van der Heijde method and Larsen's method (CRP [28], MMP-3 [29], 1CTP [30], and DAS [31]).

We showed for the first time that serum adiponectin levels were higher in the severe RA group than in control and mild RA groups. Interestingly, while other disease severity-related variables, such as MMP-3, 1CTP, DAS28-CRP, and dose of prednisolone correlated with CRP, serum adiponectin levels did not, in both the mild and severe RA groups (Table 3). It has been reported that serum TNF-α and CRP levels are elevated in RA patients [32, 33], and TNF-α, CRP, and corticosteroid markedly inhibit adiponectin gene expression in cultured adipocytes [16, 34]. Furthermore, anti-TNF-α therapy restored serum adiponectin level in RA patients [14, 15, 35]. On the other hand, despite elevated CRP levels and higher dose of treated oral prednisolone (corticosteroid), serum adiponectin levels were elevated in the severe RA group than in the mild

Table 5 Separation of mild and severe RA using a cutoff value for serum adiponectin of 18 μg/ml

	Serum adiponectin level	
	<18 μg/ml	≥18 μg/ml
Mild RA group (n)	31	6
Severe RA group (n)	27	26
% with severe RA	46.6%	81.3%

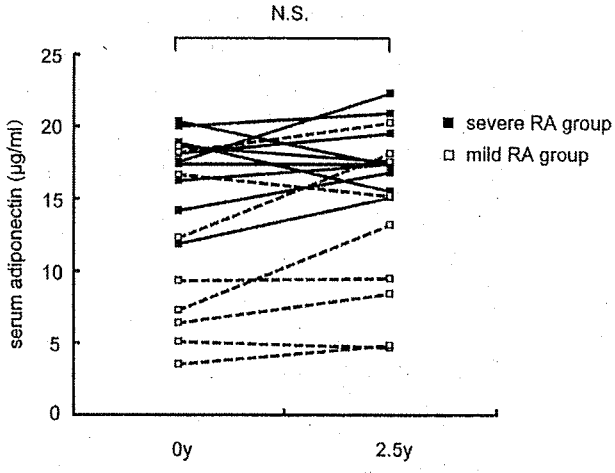

Fig. 3 Changes in serum adiponectin levels of 18 RA subjects in 2.5-year interval. The mean serum adiponectin level of the whole group was 14.0±5.5 μg/ml at baseline (0 years) and 15.2±5.2 μg/ml at follow-up (2.5 years, P=0.07); 10.8±5.8 vs. 12.4±5.8 μg/ml in mild RA group (P=0.122) and 17.2±2.7 vs. 18.0±2.4 μg/ml in severe RA group (P=0.372) and the change was not significant in either groups. None of the mild RA patients showed worsening to severe RA category during this period

RA group in the present study (Table 3). Considered together, serum adiponectin should be induced by unknown factors associated with the number of destructed joints, especially in large joints, and their effects should exceed the inhibitory effects of TNF-α, CRP, and prednisolone in RA patients. Recently, Fantuzzi [36] suggested that adiponectin promotes survival during periods of catabolism secondary to malnutrition and that hyperadiponectinemia may be the result of response to catabolic state in RA. Consequently, a catabolic state accompanied by joint destruction, especially in large joints, may be one of the strong inducer of serum adiponectin level.

It has been reported that a low BMI is a sensitive and independent predictor of radiographic progression of joint damage assessed by Larsen's method in RA [37, 38]. In this study, there was no significant difference in BMI between control, mild RA, and severe RA group (21.9±3.2 vs. 22.1± 3.4 vs. 20.8±3.0 kg/m^2). In addition, in total RA group, BMI showed only tendency of positive correlation with disease severity (P=0.059). However, under such condition, serum adiponectin levels were significantly higher in severe RA group than in the control and mild RA groups (Table 1, Fig. 1). Furthermore, multivariate logistic regression analyses revealed that even when the odds ratios were adjusted for BMI, serum adiponectin level significantly correlates with disease severity of RA (Table 4). Therefore, we speculate that serum adiponectin levels can be a better sensitive indicator of the expansion of joint destruction than BMI in RA patients. To further investigate the time course changes in serum adiponectin levels and severity of RA, 18 patients were assessed 2.5 years later. The results showed no significant change in serum adiponectin levels and none of the mild RA patients progressed to severe RA. The lack of change in the severity category during this period is compatible with previous reports indicating that most of the progression of joint damage in RA occurs during the first years of the disease and decrease thereafter [10, 11, 20]; and under such conditions, serum adiponectin level is relatively stable in established RA (disease duration ≥5 years).

For clinical translation of these findings, we determined the cutoff level of serum adiponectin level. The estimated cutoff levels estimated by the histogram of serum adiponectin level showed relatively high sensitivity (81.3%) but low specificity (53.4%) in this study (Fig. 2, Table 5), indicating that increased number of destructed joints may be one of the additive, but not a specific factor of high serum adiponectin level in RA. Consequently, prospective studies in early stage of RA (disease duration <5 years) and in large number of RA patients are needed to determine the cutoff level of adiponectin to be used as an indicator or predictor of destructed joints. In addition, to elucidate the effect of hyperadiponectinemia on the severity of RA, further animal experiments are needed.

Despite the limitation of observational study, we demonstrated that the severity of RA, evaluated by the number of destructed joints on plain radiographs detected in the whole skeleton, correlated with serum adiponectin concentrations. This finding should encourage further research to investigate the role of adiponectin in RA and design new adiponectin-based treatment strategies for RA.

Acknowledgments This work was supported by grants from the Ministry of Health, Labor, and Welfare of Japan.

Disclosures None.

References

1. Maeda N, Shimomura I, Kishida K, Nishizawa H, Matsuda M, Nagaretani H, Furuyama N, Kondo H, Takahashi M, Arita Y, Komuro R, Ouchi N, Kihara S, Tochino Y, Okutomi K, Horie M, Takeda S, Aoyama T, Funahashi T, Matsuzawa Y (2002) Diet-induced insulin resistance in mice lacking adiponectin/ACRP30. Nat Med 8:731–737
2. Matsuda M, Shimomura I, Sata M, Arita Y, Nishida M, Maeda N, Kumada M, Okamoto Y, Nagaretani H, Nishizawa H, Kishida K, Komuro R, Ouchi N, Kihara S, Nagai R, Funahashi T, Matsuzawa Y (2002) Role of adiponectin in preventing vascular stenosis. The missing link of adipo-vascular axis. J Biol Chem 277:37487–37491
3. Wulster-Radcliffe MC, Ajuwon KM, Wang J, Christian JA, Spurlock ME (2004) Adiponectin differentially regulates cytokines in porcine macrophages. Biochem Biophys Res Commun 316:924–929
4. Luo XH, Guo LJ, Yuan LQ, Xie H, Zhou HD, Wu XP, Liao EY (2005) Adiponectin stimulates human osteoblasts proliferation and differentiation via the MAPK signaling pathway. Exp Cell Res 309:99–109
5. Oshima K, Nampei A, Matsuda M, Iwaki M, Fukuhara A, Hashimoto J, Yoshikawa H, Shimomura I (2005) Adiponectin increases bone mass by suppressing osteoclast and activating osteoblast. Biochem Biophys Res Commun 331:520–526
6. Otero M, Lago R, Gomez R, Lago F, Dieguez C, Gomez-Reino JJ, Gualillo O (2006) Changes in plasma levels of fat-derived hormones adiponectin, leptin, resistin and visfatin in patients with rheumatoid arthritis. Ann Rheum Dis 65:1198–1201
7. Senolt L, Pavelka K, Housa D, Haluzik M (2006) Increased adiponectin is negatively linked to the local inflammatory process in patients with rheumatoid arthritis. Cytokine 35:247–252
8. Ehling A, Schaffler A, Herfarth H, Tarner IH, Anders S, Distler O, Paul G, Distler J, Gay S, Scholmerich J, Neumann E, Muller-Ladner U (2006) The potential of adiponectin in driving arthritis. J Immunol 176:4468–4478
9. Arita Y, Kihara S, Ouchi N, Takahashi M, Maeda K, Miyagawa J, Hotta K, Shimomura I, Nakamura T, Miyaoka K, Kuriyama H, Nishida M, Yamashita S, Okubo K, Matsubara K, Muraguchi M, Ohmoto Y, Funahashi T, Matsuzawa Y (1999) Paradoxical decrease of an adipose-specific protein, adiponectin, in obesity. Biochem Biophys Res Commun 257:79–83
10. Sharp JT, Wolfe F, Mitchell DM, Bloch DA (1991) The progression of erosion and joint space narrowing scores in rheumatoid arthritis during the first twenty-five years of disease. Arthritis Rheum 34:660–668

11. van der Heijde DM, van Leeuwen MA, van Riel PL, Koster AM, van 't Hof MA, van Rijswijk MH, van de Putte LB (1992) Biannual radiographic assessments of hands and feet in a three-year prospective followup of patients with early rheumatoid arthritis. Arthritis Rheum 35:26–34
12. Arnett FC, Edworthy SM, Bloch DA, McShane DJ, Fries JF, Cooper NS, Healey LA, Kaplan SR, Liang MH, Luthra HS et al (1988) The American Rheumatism Association 1987 revised criteria for the classification of rheumatoid arthritis. Arthritis Rheum 31:315–324
13. Ryo M, Nakamura T, Kihara S, Kumada M, Shibazaki S, Takahashi M, Nagai M, Matsuzawa Y, Funahashi T (2004) Adiponectin as a biomarker of the metabolic syndrome. Circ J 68:975–981
14. Komai N, Morita Y, Sakuta T, Kuwabara A, Kashihara N (2007) Anti-tumor necrosis factor therapy increases serum adiponectin levels with the improvement of endothelial dysfunction in patients with rheumatoid arthritis. Mod Rheumatol 17:385–390
15. Nishida K, Okada Y, Nawata M, Saito K, Tanaka Y (2008) Induction of hyperadiponectinemia following long-term treatment of patients with rheumatoid arthritis with infliximab (IFX), an anti-TNF-alpha antibody. Endocr J 55:213–216
16. Fasshauer M, Klein J, Neumann S, Eszlinger M, Paschke R (2002) Hormonal regulation of adiponectin gene expression in 3T3-L1 adipocytes. Biochem Biophys Res Commun 290:1084–1089
17. Maeda N, Takahashi M, Funahashi T, Kihara S, Nishizawa H, Kishida K, Nagaretani H, Matsuda M, Komuro R, Ouchi N, Kuriyama H, Hotta K, Nakamura T, Shimomura I, Matsuzawa Y (2001) PPARgamma ligands increase expression and plasma concentrations of adiponectin, an adipose-derived protein. Diabetes 50:2094–2099
18. Yamada S, Ano N, Toda K, Kitaoka A, Shiono K, Inoue G, Atsuda K, Irie J (2008) Telmisartan but not candesartan affects adiponectin expression in vivo and in vitro. Hypertens Res 31:601–606
19. Koshiba K, Nomura M, Nakaya Y, Ito S (2006) Efficacy of glimepiride on insulin resistance, adipocytokines, and atherosclerosis. J Med Invest 53:87–94
20. Ochi T, Yonemasu K, Iwase R, Sasaki T, Tsuyama K, Ono K (1984) Serum C1q levels as a prognostic guide to articular erosions in patients with rheumatoid arthritis. Arthritis Rheum 27:883–887
21. Steinbrocker O, Traeger CH, Batterman RC (1949) Therapeutic criteria in rheumatoid arthritis. J Am Med Assoc 140:659–662
22. Wakitani S, Murata N, Toda Y, Ogawa R, Kaneshige T, Nishimura Y, Ochi T (1997) The relationship between HLA-DRB1 alleles and disease subsets of rheumatoid arthritis in Japanese. Br J Rheumatol 36:630–636
23. Inoue E, Yamanaka H, Hara M, Tomatsu T, Kamatani N (2007) Comparison of Disease Activity Score (DAS)28- erythrocyte sedimentation rate and DAS28-C-reactive protein threshold values. Ann Rheum Dis 66:407–409
24. Toritsuka Y, Nakamura N, Lee SB, Hashimoto J, Yasui N, Shino K, Ochi T (1997) Osteoclastogenesis in iliac bone marrow of patients with rheumatoid arthritis. J Rheumatol 24:1690–1696
25. Wakitani S, Kuwata K, Imoto K, Murata N, Oonishi H, Ochi T (1998) Knee and/or hip joint destruction in rheumatoid arthritis is associated with HLA-DRB1*0405 in Japanese patients. Clin Rheumatol 17:485–488
26. Momohara S, Yamanaka H, Holledge MM, Mizumura T, Ikari K, Okada N, Kamatani N, Tomatsu T (2004) Cartilage oligomeric matrix protein in serum and synovial fluid of rheumatoid arthritis: potential use as a marker for joint cartilage damage. Mod Rheumatol 14:356–360
27. Shibuya K, Hagino H, Morio Y, Teshima R (2002) Cross-sectional and longitudinal study of osteoporosis in patients with rheumatoid arthritis. Clin Rheumatol 21:150–158
28. Jansen LM, van der Horst-Bruinsma IE, van Schaardenburg D, Bezemer PD, Dijkmans BA (2001) Predictors of radiographic joint damage in patients with early rheumatoid arthritis. Ann Rheum Dis 60:924–927
29. Young-Min S, Cawston T, Marshall N, Coady D, Christgau S, Saxne T, Robins S, Griffiths I (2007) Biomarkers predict radiographic progression in early rheumatoid arthritis and perform well compared with traditional markers. Arthritis Rheum 56:3236–3247
30. Aman S, Paimela L, Leirisalo-Repo M, Risteli J, Kautiainen H, Helve T, Hakala M (2000) Prediction of disease progression in early rheumatoid arthritis by ICTP, RF and CRP. A comparative 3-year follow-up study. Rheumatology (Oxford) 39:1009–1013
31. Welsing PM, van Gestel AM, Swinkels HL, Kiemeney LA, van Riel PL (2001) The relationship between disease activity, joint destruction, and functional capacity over the course of rheumatoid arthritis. Arthritis Rheum 44:2009–2017
32. Barrera P, Boerbooms AM, Janssen EM, Sauerwein RW, Gallati H, Mulder J, de Boo T, Demacker PN, van de Putte LB, van der Meer JW (1993) Circulating soluble tumor necrosis factor receptors, interleukin-2 receptors, tumor necrosis factor alpha, and interleukin-6 levels in rheumatoid arthritis. Longitudinal evaluation during methotrexate and azathioprine therapy. Arthritis Rheum 36:1070–1079
33. Cohick CB, Furst DE, Quagliata S, Corcoran KA, Steere KJ, Yager JG, Lindsley HB (1994) Analysis of elevated serum interleukin-6 levels in rheumatoid arthritis: correlation with erythrocyte sedimentation rate or C-reactive protein. J Lab Clin Med 123:721–727
34. Yuan G, Chen X, Ma Q, Qiao J, Li R, Li X, Li S, Tang J, Zhou L, Song H, Chen M (2007) C-reactive protein inhibits adiponectin gene expression and secretion in 3T3-L1 adipocytes. J Endocrinol 194:275–281
35. Serelis J, Kontogianni MD, Katsiougiannis S, Bletsa M, Tektonidou MG, Skopouli FN (2008) Effect of anti-TNF treatment on body composition and serum adiponectin levels of women with rheumatoid arthritis. Clin Rheumatol 27:795–797
36. Fantuzzi G (2008) Adiponectin and inflammation: consensus and controversy. J Allergy Clin Immunol 121:326–330
37. van der Helm-van Mil AH, van der Kooij SM, Allaart CF, Toes RE, Huizinga TW (2008) A high body mass index has a protective effect on the amount of joint destruction in small joints in early rheumatoid arthritis. Ann Rheum Dis 67:769–774
38. Westhoff G, Rau R, Zink A (2007) Radiographic joint damage in early rheumatoid arthritis is highly dependent on body mass index. Arthritis Rheum 56:3575–3582

Biochemical and Biophysical Research Communications 378 (2009) 186–191

Contents lists available at ScienceDirect

Biochemical and Biophysical Research Communications

journal homepage: www.elsevier.com/locate/ybbrc

Adenovirus-mediated gene transfer of adiponectin reduces the severity of collagen-induced arthritis in mice

Kosuke Ebina [a,b], Kazuya Oshima [a], Morihiro Matsuda [b,c,d], Atsunori Fukuhara [b], Kazuhisa Maeda [b], Shinji Kihara [b], Jun Hashimoto [a], Takahiro Ochi [e], Nirmal K. Banda [f], Hideki Yoshikawa [a], Iichiro Shimomura [a,*]

[a] Departments of Orthopaedics and Metabolic Medicine, Graduate School of Medicine, Osaka University, 2-2 Yamadaoka, Suita, Osaka 565-0871, Japan
[b] Metabolic Medicine, Graduate School of Medicine, Osaka University, 2-2 Yamadaoka, Suita, Osaka 565-0871, Japan
[c] Division of Analysis for Pathophysiology, Institute of Clinical Research, National Hospital Organization Kure Medical Center, Kure, Hiroshima 737-0023, Japan
[d] Department of Internal Medicine, National Hospital Organization Kure Medical Center, Kure, Hiroshima 737-0023, Japan
[e] Osaka Police Hospital, 10-31 Kitayama-cho, Tennoji-ku, Osaka 543-0035, Japan
[f] Division of Rheumatology B115, University of Colorado at Denver and Health Sciences Center, M-20 3104, 1775 North Ursula St., Aurora, CO 80045, USA

ARTICLE INFO

Article history:
Received 24 October 2008
Available online 21 November 2008

Keywords:
Adiponectin
Collagen-induced arthritis
Complement
Disease severity
Inflammation
Mice
Rheumatoid arthritis

ABSTRACT

Adiponectin (APN) is a hormone released by adipose tissue with anti-inflammatory properties. The purpose of this study was to examine the therapeutic effects of systemic delivery of APN in murine arthritis model. Collagen-induced arthritis (CIA) was induced in male DBA1/J mice, and adenoviral vectors encoding human APN (Ad-APN) or beta-galactosidase (Ad-β-gal) as control were injected either before or during arthritis progression. Systemic APN delivery at both time points significantly decreased clinical disease activity scores of CIA. In addition, APN treatment before arthritis progression significantly decreased histological scores of inflammation and cartilage damage, bone erosion, and mRNA levels of pro-inflammatory cytokines in the joints, without altering serum anti-collagen antibodies levels. Immunohistochemical staining showed significant inhibition of complement C1q and C3 deposition in the joints of Ad-APN infected CIA mice. These results provide novel evidence that systemic APN delivery prevents inflammation and joint destruction in murine arthritis model.

Rheumatoid arthritis (RA) is an autoimmune disease characterized by chronic inflammation of joint synovial tissues, followed by cartilage destruction and bone erosion. Collagen-induced arthritis (CIA) is an established rodent model of autoimmune polyarthritis with many similarities to human RA, and the immunopathological process of CIA has been reported in details [1]. Briefly, injection of chicken type II collagen (CII) in complete Freund's adjuvant (CFA) results in proliferation and differentiation of T-cells into CD4+Th1-cells in the draining lymph nodes. These cells then promote the production of anti-collagen IgG by activated CII-specific B-cells. These antibodies enter the joint and bind to CII, forming an immunocomplex (IC), which activates the complement cascade. Complement enhances the permeability of the vascular endothelium, and facilitates infiltration of monocytes (macrophages) and neutrophils into the joint. In the joint space, macrophages produce tumor necrosis factor (TNF)-α and interleukin (IL)-1. TNF-α enhances vascular permeability and migration of inflammatory cells into the joint space, and IL-1 is the primary trigger of tissue destruction by infiltrating cells and resident synoviocytes.

Adiponectin (APN) is an adipocytokine that shares strong homologies with the complement factor C1q and TNF-α [2]. APN has anti-inflammatory effects, and suppresses TNF-α and IL-6 production by macrophages activated with lipopolysaccharide (LPS) through suppression of nuclear factor-kappa B (NF-κB) signaling [3]. Accumulating evidence suggests a novel link between APN and inflammatory joint diseases. For example, APN concentration in the synovial fluid correlates negatively with synovial fluid leukocyte count in patients with RA, suggesting that APN is an anti-inflammatory molecule in RA [4]. However, APN levels in synovial fluid and serum are elevated in patients with RA compared with healthy controls [4], and APN treatment induces IL-6 production by synovial fibroblasts from RA patients [5], suggesting that APN is a pro-inflammatory molecule in RA. Thus, the effects of APN in RA are controversial. In the present study, we investigated the effects of APN on CIA mice using APN-producing adenovirus.

Materials and methods

Materials. Enzyme-linked immunosorbent assay (ELISA) for murine APN (including all isoforms) was purchased from Otsuka Pharmaceutical (Tokyo, Japan). Anti-APN polyclonal antibody used

* Corresponding author. Fax: +81 6 6879 3739.
E-mail address: ichi@imed2.med.osaka-u.ac.jp (I. Shimomura).

0006-291X/$ - see front matter © 2008 Elsevier Inc. All rights reserved.
doi:10.1016/j.bbrc.2008.11.005

for Western blotting was described previously [6]. Tartrate-resistant acid phosphatase (TRAP) staining kit was purchased from Cell Garage (Tokyo, Japan).

Induction and assessment of CIA. To induce CIA, we injected intradermally 100 μl of an emulsion containing 200 μg of chicken CII (Sigma, St. Louis, MO) and 200 μg of *Mycobacterium tuberculosis* in CFA (Chondrex, Redmond, WA) at the base of the tail of 6-week-old male DBA/1J mice (CLEA Japan, Tokyo), twice with a 21-day gap, as described previously [7]. Clinical severity of arthritis was assessed as described previously [8]. Each limb was scored, yielding a maximum possible score of 16 per mouse. Serum was collected from the tail vein at each time point.

APN adenovirus and systemic delivery in vivo. Adenovirus producing the full-length mouse APN was prepared as described previously [9]. Then, 200 μl of 2×10^8 plaque-forming units of adiponectin-producing adenovirus (Ad-APN) or control β-galactosidase-expressing adenovirus (Ad-β-gal) were injected into the jugular vein, on 19 (before arthritis progression) or 27 (during arthritis progression) days after initial injection of CII.

Determination of IgG, IgG2a, and IgG1 titers against CII and serum complement C1q and C3 levels. The total IgG anti-collagen antibody titers against chicken CII were determined through ELISA kit (Chondrex). IgG1 and IgG2a anti-collagen antibody titers against chicken CII were determined as described previously, and expressed in optical density (OD) value [10]. Serum C1q and C3 levels were determined by ELISA as described previously [11].

Histological analysis. On day 35 after initial injection of CII, joints were harvested and fixed in phosphate-buffered 4% paraformaldehyde, decalcified in 14% ethylenediaminetetraacetic acid (EDTA), and embedded in paraffin. Joint sections were stained with Safranin O and hematoxylin/eosin, and then histologically scored for inflammation, cartilage damage, and pannus formation as described previously [12]. Immunostaining for mouse IgG, C1q, C3, neutrophils, CXC chemokine ligand (CXCL)12, and APN was performed on paraffin-embedded samples with goat anti-mouse IgG (Cappel), rat anti-mouse C1q (Hycult Biotechnology b.v., Uden, Netherlands), rat anti-mouse C3 (Hycult Biotechnology), rat-anti-mouse neutrophils, (Serotec, Oxford, UK), monoclonal antihuman/mouse CXCL12 antibody (R&D Systems Inc., Minneapolis, MN), and rabbit-anti-mouse APN (Otsuka Pharmaceutical), respectively. The other steps were performed according to the instructions provided on the labeling of Vectastain Elite ABC system (Vector Laboratories, Burlingame, CA). Scoring for IgG, C1q and C3 staining on the cartilage, and CXCL12 staining on the synovium was performed as described previously [13]. The average number of infiltrating neutrophils in the synovium was determined using a modified version of the published method [14].

Quantitative real-time PCR of joint samples. Total RNA was extracted by pulverizing the frozen individual fore paws with an RNA STAT-60 kit. The first-strand cDNA was synthesized using ThermoScript RT-PCR System (Invitrogen, San Diego, CA). Real-time polymerase chain reaction (PCR) was performed on a Light Cycler using the Fast Start DNA Master SYBR Green I (Roche Diagnostics, Indianapolis, IN). The sequences of primers were designed based on a previous report [13], and other primers are listed in Supplementary Table 1.

Lymph node cell proliferation assay. In vitro proliferation of draining lymph node (DLN) cells was examined by Cell Proliferation ELISA Bromodeoxyuridine (BrdU) kit (Roche) using a modified version of the published method [10].

Cytokine production by cultured splenocytes. Spleens were removed and cell suspensions (2×10^6 cells/well) were distributed to flat bottom 96-well plates. Spleen cells were cultured without or with either 50 μg/ml heat-denatured chicken CII (Sigma–Aldrich) or 5 μg/ml LPS from *Escherichia coli* (Sigma–Aldrich). After 48-h incubation, the supernatants were collected, and TNF-α and IL-1β levels were measured using ELISA kit (Quantikine Mouse ELISA kit, R&D Systems Inc.).

Skeletal morphology. Three-dimensional microcomputed tomography (3D-μCT) scan for ankle joints was undertaken and the trabecular bone area (percentage of bone volume [BV] per tissue volume [TV]) of distal tibia was measured using a composite X-ray analysis system (Shimadzu, SMX-100CT-SV, Kyoto, Japan).

Statistical analysis and ethical considerations. Data were expressed as means ± standard error of the mean. Differences between groups were examined for statistical significance using Chi-square test, Student's *t* test, or analysis of variance with Fisher's protected least significant difference test. A *P* value less than 0.05 denoted the presence of a statistically significant difference. The experimental protocol was approved by the Ethics Review Committee for Animal Experimentation of Osaka University School of Medicine.

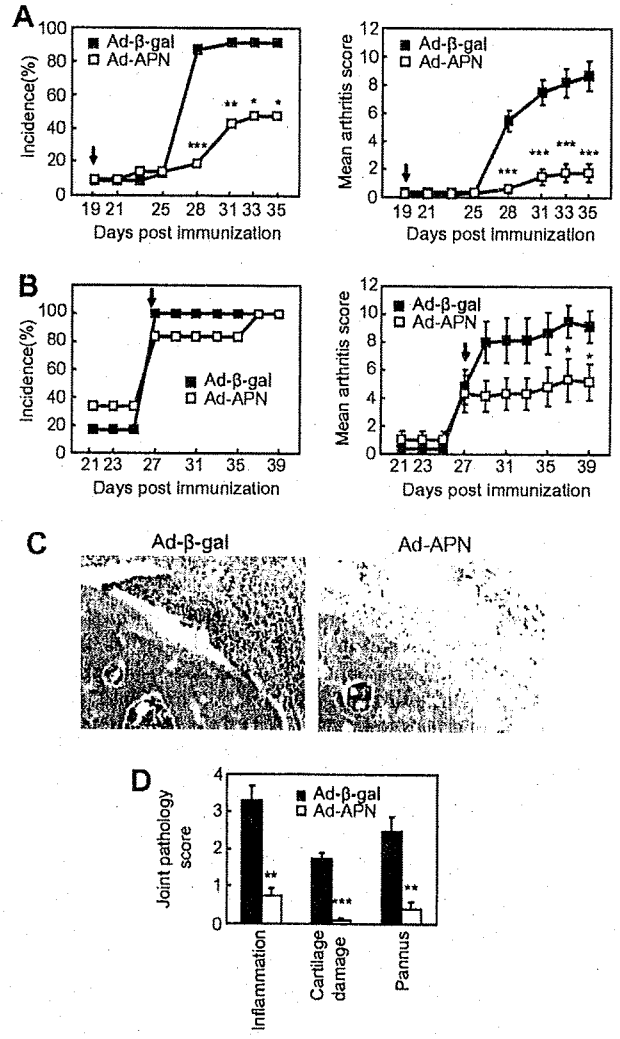

Fig. 1. Systemic delivery of APN in collagen-induced arthritis (CIA) mouse model and histological analysis of the joints. (A) On day 19, before arthritis progression, mice were injected with adenoviral vector directing the expression of either *lacZ* gene (Ad-β-gal) or APN (Ad-APN) intravenously ($n = 23$ Ad-β-gal-infected mice, $n = 21$ Ad-APN-infected mice). (B) On day 27, during arthritis progression, mice were injected with the same adenovirus ($n = 6$ mice in each group). (C) Histological features of representative hematoxylin and eosin-stained sections of the ankle joints (original magnification 200×), and (D) mean pathological scores of the joints of adenovirus-infected CIA mice ($n = 36$ joints in each group). $^{*}P < 0.05$, $^{**}P < 0.01$, $^{***}P < 0.001$, versus Ad-β-gal-infected CIA mice.

Results

Ad-APN suppresses progression of arthritis in CIA model

First, we tried two protocols to evaluate the effect of Ad-APN on CIA. When the virus was injected on day 19 (Fig. 1A), the incidence and disease activity on day 35 were significantly suppressed by Ad-APN treatment compared with Ad-β-gal (arthritis score: Ad-APN-infected mice: 1.76 ± 0.63, Ad-β-gal-infected mice: 8.68 ± 1.06; $P < 0.001$). In addition, when the virus was injected on day 27 (Fig. 1B), disease activity was significantly suppressed on day 39 by Ad-APN treatment compared with Ad-β-gal (arthritis score: Ad-APN-infected mice: 5.17 ± 1.25, Ad-β-gal-infected mice: 9.17 ± 1.15; $P < 0.05$). For the rest of this study, we used the former protocol (Fig. 1A). Histological analysis of the ankle joint showed typical features of active arthritis in Ad-β-gal-infected CIA mice, including infiltration of inflammatory cells into the synovium, cartilage damage, and pannus formation. These changes were significantly less pronounced in Ad-APN-infected CIA mice (Fig. 1C and D).

Ad-APN increases APN protein in serum and bone marrow, and does not alter serum anti-collagen antibodies or complement levels

In the experiments described in Fig. 1A, injection of Ad-APN resulted in about 5-fold increase on day 21 and about 30-fold increase on day 35 in serum APN levels (Fig. 2A). The high serum APN protein levels in Ad-APN-infected CIA mice were mainly composed of high- and middle-molecular weight forms of APN (Fig. 2B). Moreover, Ad-APN substantially increased APN protein content in knee joints compared with Ad-β-gal (Fig. 2C). Immunohistochemical staining of knee joints with anti-APN antibody indicated accumulation of APN in the bone marrow but not on the cartilage surface in Ad-APN-infected CIA mice (Fig. 2D). Under such conditions, anti-CII IgG, IgG2a, and IgG1 titers, serum C1q and C3 levels were not different between Ad-APN- and Ad-β-gal-infected CIA mice (Fig. 2E and F).

Treatment of CIA mice with Ad-APN suppresses local deposition of C1q and C3, infiltration of neutrophil, and changes in mRNAs of pro-inflammatory genes

Next, we examined the accumulation of IgG, C1q, and C3 on the cartilage of wrist, knee, and ankle joints by immunohistochemical staining (Fig. 3A and B). Under the conditions with minimum background staining, IgG deposition on the cartilage was observed in both adenovirus-infected CIA mice. On the other hand, C1q and C3 deposits on the cartilage were significantly suppressed by Ad-APN treatment compared with Ad-β-gal. Furthermore, neutrophil infiltration and synovium deposition of CXCL12, a chemokine that promotes leukocyte migration, were also significantly decreased in Ad-APN-infected CIA mice (Fig. 3A and B). To assess the inflammatory status, mRNA levels of pro-inflammatory genes, complement factors, and F4/80 (a marker of monocyte/macrophage linage) were measured in isolated forepaws. The expression levels of IL-1β, IL-6, COX-2 IFN-γ, TNF-α, C1q, C3, and F4/80 were all significantly decreased by Ad-APN treatment (Fig. 3C).

Effects of Ad-APN on immunocyte activities in lymph nodes and spleen, and bone erosion of CIA mice

Next, activities of immunocytes were measured. DLN cells from Ad-APN-infected CIA mice showed marginally inhibited proliferation activities (Fig. 4A). Splenocytes from Ad-APN-infected CIA

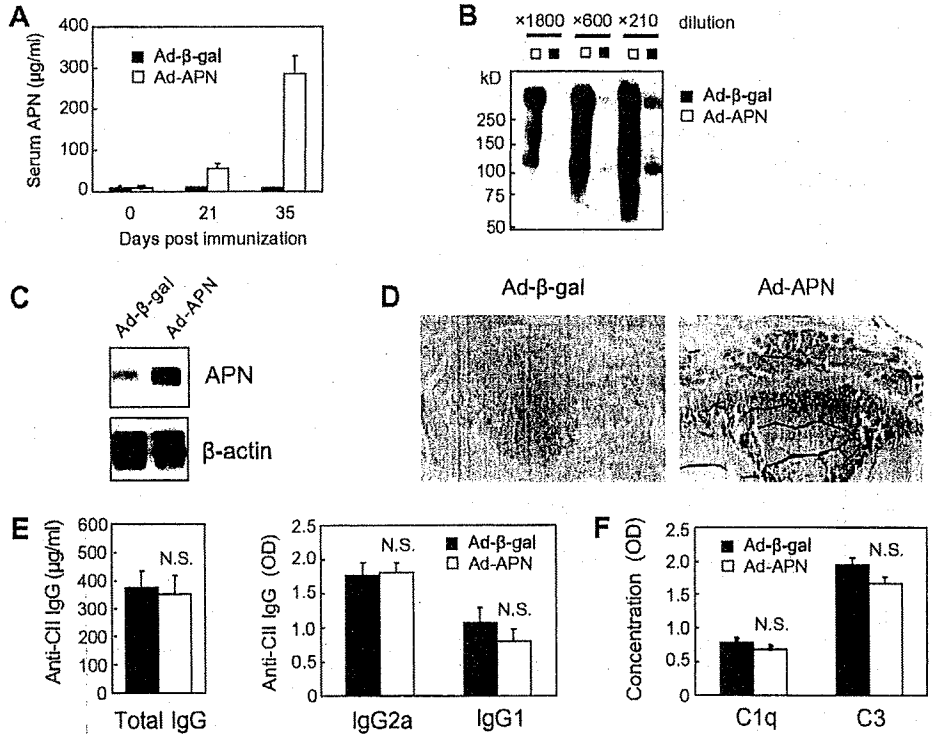

Fig. 2. High APN levels in serum and joints do not alter serum levels of anti-CII antibody, complement C1q, or C3 in CIA mice. (A) Serum APN concentrations at each time point were determined by ELISA ($n = 6$ in each group). Representative serum samples (B) and protein lysates prepared from knee joints (C) of adenovirus-infected CIA mice on day 35 were subjected sodium dodecyl sulfate-polyacrylamide gel electrophoresis without reducing reagent, and analyzed by western blot using anti-APN antibody. (D) Representative sections of proximal tibia immunostained with APN (original magnification 40×). Serum samples were obtained on day 35, and anti-CII specific IgG, IgG2a, and IgG1 levels (E), and complement C1q and C3 levels (F) were measured by ELISA ($n = 6$ in each group). NS = not significant.

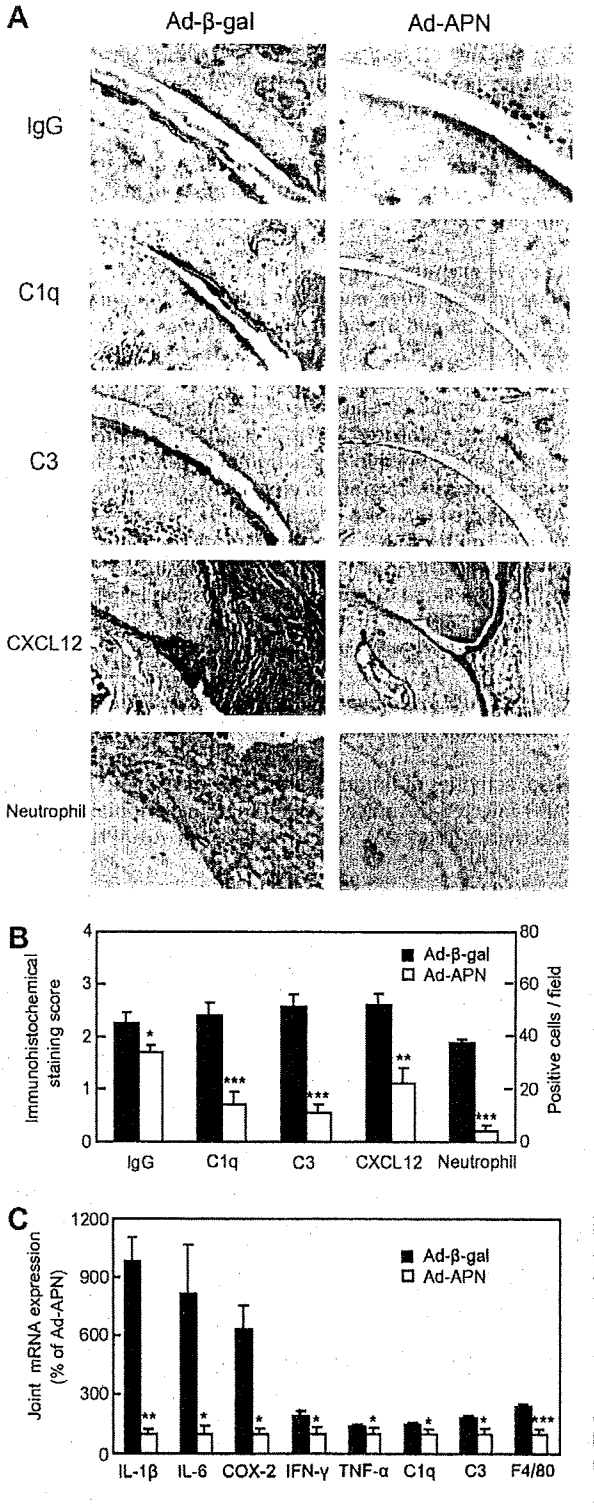

Fig. 3. Ad-APN inhibits complement deposition/expression and pro-inflammatory cytokine/enzyme expression in CIA mice. (A) Representative sections immunostained for IgG, C1q, C3, CXCL12, and neutrophil on the cartilage surface and synovium of the ankle joints of adenovirus-infected CIA mice (original magnification 200×). (B) Scoring of immunostained joint sections from adenovirus-infected CIA mice ($n = 16$ joints in each group). (C) mRNA expression levels in forepaws of adenovirus-infected CIA mice. ($n = 6$ joints in each group). Values are normalized to the level of 36B4 mRNA. $^{*}P < 0.05$, $^{**}P < 0.01$, $^{***}P < 0.001$, versus Ad-β-gal-infected CIA mice.

mice produced less IL-1β in all conditions, and less TNF-α in response to LPS *in vitro* (Fig. 4B). Finally, analysis of bone erosion of the distal tibia using μCT revealed that trabecular bone volume were significantly decreased in Ad-β-gal-infected CIA mice compared to those in Ad-APN-infected CIA mice (Fig. 4C). In addition, the number of TRAP-positive cells was significantly decreased in ankle joints of Ad-APN-infected CIA mice (Fig. 4D).

Discussion

In the present study, we demonstrated for the first time that Ad-APN significantly improved joint inflammation and bone erosion in CIA mice. There were no significant differences in anti-CII IgG, C1q, and C3 levels between Ad-APN and Ad-β-gal infected CIA mice (Fig. 2E and F), indicating that Ad-APN has little effect on humoral immunity. On the other hand, C1q and C3 deposition were markedly suppressed on the cartilage surface of Ad-APN-infected CIA mice (Fig. 3A and B). Therefore, we investigated the direct effect of APN on complement activation. APN has a substantial sequence similarity to C1q, and also binds to C1q receptor [15]. In addition, we confirmed the binding between human recombinant APN from mammalian cells and human C1q *in vitro* as reported previously [16]. However, in our preliminary experiments, this recombinant APN did not alter C1q binding to adherent CII-IC [11], CII-IC-induced mouse serum C3 activation (mainly involves classical pathway) [11], or zymosan-induced mouse serum C3 activation (mainly involves alternative pathway) [10] *in vitro* (data not shown). To elucidate the direct effect of APN on the complement activation, further *in vivo* and *in vitro* analyses are required.

We showed marked suppression of C1q and C3 deposition, accompanied by significant downregulation of C1q, C3, and F4/80 mRNAs in the Ad-APN-infected CIA joints (Fig. 3). A previous report demonstrated that APN inhibited the expression of endothelial adhesion molecules induced by TNF-α, and consequent transendothelial migration of monocytes [17]. In addition, TNF-α-induced vascular permeability is required for the migration of inflammatory cells into the joint and development of inflammatory process in mouse arthritis models [1], and APN was reported to inhibit TNF-α-induced hyperpermeability in endothelial cells [18]. Our group demonstrated that APN was protective against murine colitis through inhibition of macrophages infiltration and release of pro-inflammatory cytokines [19]. Considering that C1q is mainly produced by monocyte/macrophage linage [20], and C3 is produced by liver and inflamed synoviocytes [21], reduced accumulation of F4/80 positive cells and consequent C3 production by inflamed synovium should result in suppression of complement deposition and pro-inflammatory cytokine production in the CIA joints.

We also observed that Ad-APN suppressed synovial deposition of CXCL12. CXCL12 is a chemokine anchored to heparan sulfate (HS) proteoglycans on endothelial cells of RA synovium [22], and acts as a critical chemoattractant in the pathogenesis of CIA [23]. APN inhibits the binding of CXCL12 to HS, and alters the distribution of CXCL12 at the site of inflammation [24]. Taken together, Ad-APN may improve joint inflammation through decreased CXCL12 deposition in CIA synovium.

Previous studies showed that the cellular immunity, represented by the activity of immunocytes of lymph nodes or spleen, is causally associated with the disease activity in CIA mice [25]. In this study, Ad-APN marginally reduced DLN cells proliferation (Fig. 4A), and significantly suppressed IL-1β production and TNF-α production from splenocytes (Fig. 4B). These results indicate that Ad-APN could suppress disease activity of CIA partially through inhibition of cellular immunity.

In this study, Ad-APN reduced the number of TRAP-positive cells and resulted in amelioration of bone erosion in the joints of CIA mice (Fig. 4C and D). Previously, we and others reported that